Oral carcinoma: Clinical evaluation using diffusion kurtosis imaging and its correlation with histopathologic findings

Oral carcinoma: clinical evaluation using diffusion kurtosis imaging and its correlation with histopathologic findings [1]

Ichiro Yamada [a,*], Norio Yoshino [b], Keigo Hikishima [c], Junichiro Sakamoto [b], Misaki Yokokawa [d], Yu Oikawa [d], Hiroyuki Harada [d], Tohru Kurabayashi [b], Yukihisa Saida [a], Ukihide Tateishi [a], Akane Yukimori [e], Toshiyuki Izumo [e], Shun Asahina [f]

[a] Department of Diagnostic Radiology and Nuclear Medicine, Graduate School, Tokyo Medical and Dental University, Tokyo, Japan
[b] Department of Oral and Maxillofacial Radiology, Tokyo Medical and Dental University, Tokyo, Japan
[c] Okinawa Institute of Science and Technology Graduate University, Okinawa, Japan
[d] Department of Oral and Maxillofacial Surgery, Tokyo Medical and Dental University, Tokyo, Japan
[e] Department of Oral Pathology, Tokyo Medical and Dental University, Tokyo, Japan
[f] Siemens Healthcare K.K., Tokyo, Japan

Footnotes

[1] Conflicts of Interest and Sources of Funding: For all the authors listed, no conflicts are declared. Dr. Yamada has received the Grant-in-Aid for Scientific Research (C) of MEXT, Japan (15K09915).

* Corresponding author at: Department of Diagnostic Radiology and Nuclear Medicine, Graduate School, Tokyo Medical and Dental University, 1-5-45 Yushima, Bunkyo-ku, Tokyo 113-8519, Japan.

E-mail: yamada.crad@tmd.ac.jp (I. Yamada).

Address for correspondence:
Ichiro Yamada, MD,
Department of Diagnostic Radiology and Nuclear Medicine,
Graduate School, Tokyo Medical and Dental University,
1-5-45 Yushima, Bunkyo-ku, Tokyo 113-8519, Japan.
Telephone: 81-3-5803-5310. FAX: 81-3-5803-0147.
E-mail: yamada.crad@tmd.ac.jp

ABSTRACT

Purpose: In this study, we aimed to determine the usefulness of diffusion kurtosis imaging (DKI) as a noninvasive method for evaluation of the histologic grade and lymph node metastasis in patients with oral carcinoma.

Materials and methods: Twenty-seven patients with oral carcinoma were examined with a 3-T MR system and 16-channel coil. DKI data were obtained by a single-shot echo-planar imaging sequence with repetition time, 10000 ms; echo time, 94 ms; field of view, 250 × 204.25 ms; matrix, 120 × 98; section thickness, 4 mm; four b values of 0, 500, 1000, and 2000 s/mm^2; and motion-probing gradients in three orthogonal directions. Diffusivity (D) and kurtosis (K) were calculated using the equation: $S = S_0 \bullet \exp(-b \bullet D + b^2 \bullet D^2 \bullet K/6)$. Conventional apparent diffusion coefficient (ADC) was also calculated. The MR images were compared with the histopathologic findings.

Results: Relative to the histologic grades (Grades 1, 2, and 3) of the 27 oral carcinomas, D values showed a significant inverse correlation ($r = -0.885$; $P < 0.001$) and K values showed a significant positive correlation ($r = 0.869$; $P < 0.001$), whereas ADC values showed no significant correlation ($r = -0.311$; $P = 0.115$). When comparing between metastatic and non-metastatic lymph nodes, significant differences in the D values ($P < 0.001$) and K values ($P < 0.001$), but not the ADC values ($P = 0.110$) became apparent.

Conclusions: In patients with oral carcinoma, DKI seems to be clinically useful for the evaluation of histologic grades and lymph node metastasis.

Keywords: Oral carcinoma; Diffusion kurtosis imaging; Diffusion-weighted imaging; MR imaging

1. Introduction

Oral carcinoma is one of the most common and fatal malignant neoplasms worldwide [1-3]. The prognosis of patients with oral carcinoma strictly depends on the histologic grade, as well as on the presence and extent of lymph node metastasis; therefore, accurate preoperative assessment of these prognostic factors has a definitive impact on the selection of the optimal therapy for oral carcinoma [2,3]. Preoperative staging of oral carcinoma is currently performed on the basis of computed tomography (CT), ultrasound (US), and magnetic resonance (MR) imaging; however, the histologic grade and lymph node metastasis cannot be reliably assessed by these methods. CT has poor soft tissue contrast and indeterminate size criteria [4,5]. US carries several inherent problems, including high operator dependency, artifactual interface echoes, and a limited sonographic range [6,7]. MR imaging is an alternative to CT and US, but conventional MR imaging remains incapable of evaluating the histologic grade and lymph node metastasis in oral carcinoma [8,9].

Previous reports have shown that the findings of non-Gaussian diffusion kurtosis imaging (DKI) were associated with this histologic grade of gliomas, prostate cancer, and breast cancer [10-14]. Furthermore, Yamada et al. [15,16] have recently demonstrated that non-Gaussian q-space imaging (QSI) was useful for ex vivo evaluation of the histologic grade and lymph node metastasis in esophageal and gastric carcinomas. To the best of our knowledge, however, there have been no reports on the use of non-Gaussian DKI to evaluate patients with oral carcinoma in terms of the histologic grade and lymph node metastasis.

The purposes of this study were to prospectively examine patients with oral carcinoma and to assess the usefulness of DKI as a noninvasive method of evaluating the histologic grade of oral carcinomas and detecting the presence of lymph node metastasis.

2. Materials and methods

2.1. Study population

Our institutional review board provided official approval for this study, and all patients provided written informed consent prior to participating in this study. We studied 27 consecutive patients with histologically confirmed oral squamous cell

carcinoma and who underwent oral and maxillofacial surgery at our department. Fifteen men and 12 women with a mean age of 63.6 ± 12.4 years (range, 43−82 years) participated in our study. The location of the oral carcinomas was the tongue in 16 patients (59.3%), upper gingiva in 5 patients (18.5%), lower gingiva in 5 patients (18.5%), and floor of the mouth in 1 patient (3.7%). All patients underwent MR imaging, including DKI, for preoperative evaluation.

2.2. Imaging technique

A 3-T MR imaging unit (Magnetom Spectra; Siemens, Erlangen, Germany), which was equipped with actively shielded gradients with a maximum strength of 33 mT/m, was used to perform all MR imaging scans using a 16-channel head and neck coil.

DKI data sets were obtained in the axial plane using a spin echo-based, single-shot, echo-planar imaging sequence with fat suppression by short tau inversion recovery (STIR) and the following parameters: repetition time (TR), 10000 ms; echo time (TE), 94 ms; field of view (FOV), 250 × 204.25 mm; matrix, 120 × 98; section thickness, 4 mm without intersection gaps; voxel size, 17.37 mm^3; and number of signal averaged (NSA), 1. The diffusion gradients were applied in three orthogonal directions with a duration time (δ) of 30.4 ms, a separation time (Δ) of 42.9 ms, effective diffusion time ($\Delta_{eff} = \Delta - \delta/3$) of 32.8 ms, and four different gradient strengths (g mT/m). The resulting four b values were 0, 500, 1000, and 2000 s/mm^2. The acquisition time for the DKI was 2 minutes 10 seconds.

Although the kurtosis assessment of the diffusion tensor, or diffusion kurtosis tensor imaging (DKTI), requires diffusion images in al least 15 different directions, DKI of the body can be performed based on a directionless “trace” of the diffusion tensor, which requires acquisition of only three directions [12,13]. Thus, we performed the DKI using four b values of 0, 500, 1000, and 2000 s/mm^2 in three orthogonal directions.

The standard MR imaging protocol for oral carcinoma patients at our institution included T1-weighted turbo spin-echo (TSE) imaging (TR/TE, 650/10 ms; turbo factor, 3; NSA, 1) in the axial and coronal planes; T2-weighted TSE imaging (TR/TE, 5000/94; turbo factor, 14; NSA, 1) with fat suppression by the two-point Dixon technique in the axial plane; and T2-weighted TSE imaging (TR/TE, 5400/89 ms; turbo factor, 12; NSA, 1) with fat suppression by chemical-shift selective saturation in

the coronal plane. After intravenous administration of 0.1 mmol/kg gadobutrol (Gadovist; Bayer Yakuhin, Osaka, Japan), T1-weighted TSE images (TR/TE, 640/12; turbo factor, 3; NSA, 1) with fat suppression by the two-point Dixon technique were also obtained in the axial and coronal planes. The T1-weighted, T2-weighted, and contrast-enhanced T1-weighted images were obtained with FOV of 230 × 187 mm, matrix of 384 × 312, and section thickness of 4 mm, with an intersection gap of 1 mm.

2.3. Image processing

On the basis of the DKI theory [17,18], we analyzed the signal intensity decay and calculated the DKI parameters for each voxel using the following equation:

$$S = S_0 \bullet \exp(-b \bullet D + b^2 \bullet D^2 \bullet K/6),$$

where S_0 and S represent the signal intensities at a b value of 0 s/mm^2 and at b values other than 0 s/mm^2, respectively; D stands for the diffusivity (× 10^{-3} mm^2/s); and K stands for the kurtosis [arbitrary unit (a.u.)]. D represents the diffusion coefficient corrected for non-Gaussian bias, and K represents deviation from the Gaussian behavior [17,18]. In addition, the conventional apparent diffusion coefficient (ADC) was also calculated for each voxel according to the following equation:

$$S = S_0 \bullet \exp(-b \bullet ADC).$$

D, K, and ADC maps were generated using signal intensities on a pixel-by-pixel basis at b values of 0, 500, 1000, and 2000 s/mm^2. All image processing was performed by an in-house program developed with MatLab software (R2015a; MathWorks, Natick, MA) [19].

2.4. Image analysis

Two observers, who were blinded to the histologic analyses, independently evaluated the MR images for each patient. Disagreements on any findings were resolved by discussion and consensus. The MR images of the primary tumor and lymph nodes were reviewed in terms of size, signal intensity, and border contour. Each MR image of the primary tumor and lymph nodes was compared with the corresponding histopathologic findings.

For the D, K, and ADC maps, regions of interest (ROIs), which were approximately equivalent in size to the tumor or lymph node cross-sectional area, were drawn by one observer on the primary tumor and lymph nodes using the T1-weighted, T2-weighted, and contrast-enhanced T1-weighted images as references. Using the ImageJ 1.47 software program (National Institutes of Health, Bethesda, MD, USA), the mean values of all three or four ROIs were calculated for each tumor and lymph node to generate the D, K, and ADC values. The values were taken from three-dimensional volumes that consisted of three or four slices depending on tumor size, which was intended to give full tumor coverage. Finally, the MR findings of all patients were compared with the corresponding histologic findings using visual and spatial matching of anatomic features.

2.5. Histologic preparation and examination

After surgery, all the primary tumors and lymph nodes were subjected to histopathologic examination. The histologic sections were paraffin-embedded and cut with a microtome into 6-μm-thick slices. After staining with hematoxylin-eosin (H-E), one experienced pathologist who was blinded to the MR results evaluated all the specimens to determine the depth of tumor invasion. Subsequently, the pathologist classified the histologic grade of the oral squamous cell carcinomas as Grade 1 (well-differentiated), Grade 2 (moderately differentiated), or Grade 3 (poorly differentiated), based on the World Health Organization grading criteria [1-3]; the presence or absence of lymph node metastasis was also determined.

2.6. Statistical analysis

The means ± standard deviations (SD) of the D, K, and ADC values of the oral carcinomas and lymph nodes were calculated from the corresponding maps. Data were analyzed using IBM SPSS Statistics, version 20 (IBM SPSS Japan, Tokyo, Japan) and MedCalc, version 17.9.7 (MedCalc Software, Ostend, Belgium). Correlations of the histologic grades of the oral carcinomas with the D, K, and ADC values were assessed by the Spearman’s rank correlation coefficient and the Mann-Whitney U-test. The D, K, and ADC values were compared between the metastatic and non-metastatic lymph nodes using the Mann-Whitney U-test.

Receiver operating characteristic (ROC) curve analyses were conducted to assess and compare the D, K, and ADC values in terms of their utility in

differentiating the histologic grades of oral carcinomas and in differentiating metastatic from non-metastatic lymph nodes. For the ROC curve analyses, the optimal threshold of each parameter was determined as the value that would maximize the average of sensitivity and specificity. A P value < 0.05 was considered to indicate statistical significance.

3. Results

3.1. D, K, and ADC values of oral carcinomas

In all 27 oral carcinomas, the calculated means were $1.803 \pm 0.317 \times 10^{-3}$ mm^2/s for the D values; 0.817 ± 0.114 a.u. for K values; and $0.781 \pm 0.073 \times 10^{-3}$ mm^2/s for the ADC values. The non-Gaussian D values of the oral carcinomas were significantly larger than the conventional Gaussian ADC values ($P < 0.001$). This was due to the fact that the D value represented the diffusion coefficient corrected for the non-Gaussian bias [17,18], thereby, demonstrating that the effect of non-Gaussian diffusion considerably contributed to the D values of the oral carcinomas. Similarly, since a K value of 0 indicates a perfectly Gaussian diffusion [17,18], the larger K values of the oral carcinomas implied a greater deviation of diffusion from a perfectly Gaussian behavior.

3.2. Histologic grades of oral carcinomas on DKI maps

Next, we investigated the association of the histologic grades of the oral carcinomas with the DKI parameters that were found to be related with the non-Gaussianity, as mentioned in the previous section. Histopathologic examination of the 27 oral squamous cell carcinomas showed that 13 carcinomas were Grade 1, 11 carcinomas were Grade 2, and 3 carcinomas were Grade 3.

As shown in Table 1 and Figure 1, a significant inverse correlation was found between the D values and the histologic grades of the oral carcinomas ($r = -0.885$; $P < 0.001$) (Grade 1 vs. Grade 2, $P < 0.001$; Grade 1 vs. Grade 3, $P < 0.001$; Grade 2 vs. Garde3, $P = 0.011$). The K values were also significantly positively correlated with the histologic grades of the oral carcinomas ($r = 0.869$; $P < 0.001$) (Grade 1 vs. Grade 2, $P < 0.001$; Grade 1 vs. Grade 3, $P < 0.001$; Grade 2 vs. Garde3, $P = 0.001$). However, no significant correlation was found between the ADC values and the histologic grades of the oral carcinomas ($r = -0.311$; $P = 0.115$) (Grade 1 vs. Grade 2, $P = 0.138$; Grade 1 vs. Grade 3, $P = 0.743$; Grade 2 vs. Garde3, $P = 0.863$).

Representative cases with Grade 1 and Grade 3 oral carcinoma are shown in Figures 2 and 3 respectively. These data indicated that it is possible to differentiate the histology grades of oral carcinomas on the basis of the non-Gaussian DKI parameters.

3.3. Lymph node metastasis from oral carcinoma on DKI maps

We investigated the association between lymph node status in patients with oral carcinoma and the non-Gaussian DKI parameters. Lymph node metastasis was found in 10 of 27 patients; each histologically confirmed lymph node (11 metastatic and 16 non-metastatic) was compared with the DKI parameters on a node-by-node basis.

As shown in Table 2 and Figure 4, the D values of the metastatic lymph nodes were significantly lower than those of the non-metastatic lymph nodes ($1.351 \pm 0.285 \times 10^{-3}$ mm^2/s vs. $2.054 \pm 0.333 \times 10^{-3}$ mm^2/s; $P < 0.001$). Likewise, the K values of the metastatic lymph nodes were statistically significantly higher than those of the non-metastatic lymph nodes (1.079 ± 0.182 a.u. vs. 0.775 ± 0.078 a.u.; $P < 0.001$). However, no significant differences in the ADC values were found between the metastatic and non-metastatic lymph nodes ($0.741 \pm 0.054 \times 10^{-3}$ mm^2/s vs. $0.771 \pm 0.039 \times 10^{-3}$ mm^2/s; $P = 0.110$).

Representative cases with non-metastatic and metastatic lymph nodes are shown in Figures 5 and 6 respectively. These data indicated that it is possible to differentiate between metastatic and non-metastatic lymph nodes in patients with oral carcinoma on the basis of the non-Gaussian DKI parameters.

3.4. ROC curve analyses of the D, K, and ADC values

In Table 3 and Figure 7a the results of the ROC curve analyses of the D, K, and ADC values for differentiating Grade 2 or Grade 3 from Grade 1 oral carcinomas are shown. Compared with the area under the curve (AUC) for the ADC values (0.714), the AUCs for the D values (0.989; $P = 0.0115$) and the K values (0.978; $P = 0.0089$) were significantly larger. There was no significant difference in the AUCs between the D values and the K values ($P = 0.6774$). Table 4 and Figure 7b show the results of the ROC curve analyses for differentiating Grade 3 from Grade 1 or Grade 2 oral carcinomas. The AUCs for the D values (0.986) and the K values (0.986) were also larger than the AUC for the ADC values (0.514), although there was no

significant difference. Therefore, a cut-off D value of ≤ 1.881 × 10^{-3} mm^2/s and a cut-off K value of > 0.814 a.u. seem to be useful for differentiating Grade 2 or Grade 3 from Grade 1 oral carcinomas; a cut-off D value of ≤ 1.457 × 10^{-3} mm^2/s and a cut-off K value of > 0.893 a.u. may be useful for differentiating Grade 3 from Grade 1 or Grade 2 oral carcinomas.

Table 5 and Figure 7c demonstrate the results of the ROC curve analyses of the D, K, and ADC values for differentiating between metastatic and non-metastatic lymph nodes in patients with oral carcinoma. The AUCs for the D values (0.938; P = 0.0132) and the K values (0.977; P = 0.0077) were significantly higher than the AUC for the ADC values (0.688). There was no significant difference in the AUCs between the D values and K values (P = 0.5249). Therefore, a cut-off D value of ≤ 1.419 × 10^{-3} mm^2/s and a cut-off K value of > 0.834 a.u. seem to be useful for differentiating metastatic from non-metastatic lymph nodes in patients with oral carcinoma.

4. Discussion

Conventional diffusion-weighted imaging (DWI) assumes Gaussian behavior of water diffusion, so that the distribution of water displacement follows a statistically similar distribution to free diffusion and that the diffusion-weighted signal attenuations are monoexponential with the b values. However, the complex structure of most tissues, which comprise various types of cells and their membranes, can cause substantial deviation of the distribution of diffusion displacement from a Gaussian form. A non-Gaussian model of DWI, DKI was first proposed by Jensen et al. [17] for the investigation of neurologic pathologies. Since DKI can quantify the deviation of diffusion from a Gaussian behavior in tissues with restricted water diffusion, it is able to more accurately reflect the microstructural complexity of tissues, compared with conventional DWI [17,18]. As previously reported, DKI exhibited promising results in evaluating gliomas, prostate cancer, and breast cancer, and DKI-derived parameters have been shown to have a highly positive association with the histologic grades of the carcinomas [10-14]. Furthermore, Yamada et al. [15,16] have demonstrated ex vivo that QSI, which is another non-Gaussian model of DWI, was useful for evaluating the histologic grade and lymph node metastasis of esophageal and gastric carcinomas. Therefore, we hypothesized that DKI might be more effective than conventional DWI for the assessment of oral carcinomas in terms of the histologic

grades and lymph node metastasis.

In the present study on 27 oral carcinoma cases, the mean values calculated and derived from the DKI data were $1.803 \pm 0.317 \times 10^{-3}$ mm^2/s for the D values, 0.817 ± 0.114 a.u. for the K values, and $0.781 \pm 0.073 \times 10^{-3}$ mm^2/s for the ADC values. The non-Gaussian D values of the oral carcinomas were found to be significantly larger than the conventional Gaussian ADC values. Because the D value represents the diffusion coefficient corrected for a non-Gaussian bias [17, 18], these data demonstrate the substantial contribution of the effect of non-Gaussian diffusion to the D values of oral carcinomas. Similarly, since a K value of zero indicates perfectly Gaussian diffusion [17,18], the larger K values of the oral carcinomas implies a greater deviation of diffusion from perfectly Gaussian behavior. These tendencies were compatible with the results of previous reports that dealt with other organs [12]. Moreover, the significant increase in the D values compared with the ADC values has been observed in a variety of other tissues [12-14].

Our data revealed significant correlations between the DKI parameters and the histologic grades of oral carcinomas. Previous studies have shown correlations between the kurtosis obtained by DKI and the histologic grades of cerebral gliomas, prostate cancer, and breast cancer [10-14]; in particular, kurtosis measured by DKI increased with the aggressiveness of the tumor, probably because of the greater microstructural complexity of higher-grade tumors [12]. Because DKI is exquisitely sensitive to changes in tissue microstructure [17,18], it could be an effective method for noninvasive assessment of the histologic grades of oral carcinomas. Previous studies have shown that differentiation among histologic tumor grades based on conventional ADC values is often difficult because of the considerable overlap among the ADC values of different histologic tumor grades [20-22]. Therefore, DKI might be more accurate than conventional DWI in differentiating the histologic tumor grades of oral carcinomas.

Our results of the ROC curve analyses for differentiating the histologic grades of oral carcinomas demonstrated that the AUCs for D values and K values were significantly greater than the AUC for ADC values. Furthermore, the cut-off D value and the cut-off K value were found to be useful for differentiating Grade 2 or Grade 3 from Grade 1 oral carcinomas and for differentiating Grade 3 from Grade 1 or Grade 2 oral carcinomas.

Our findings demonstrated that DKI allows differentiation between metastatic

and non-metastatic lymph nodes in patients with oral carcinoma. Previous reports have indicated that evaluation of lymph node metastasis in patients with oral carcinoma is challenging for any imaging modality because nodal size alone is not a reliable diagnostic criterion for lymph node metastasis [4-9]. Similar to the limitations of the ADC values in the evaluation of histologic tumor grades mentioned above, results of recent studies have shown that although ADC values may be useful for evaluating lymph node metastasis, differentiation between metastatic and non-metastatic lymph nodes was likewise difficult for the same reasons [23-26]. On the other hand, DKI might be a useful tool for noninvasive assessment of lymph node metastasis in patients with oral carcinoma because it is potentially sensitive to aspects of this microstructural complexity. In this respect, Yamada et al. [15,16] have recently demonstrated that QSI was also useful for differentiating metastatic from non-metastatic lymph nodes in esophageal and gastric carcinomas ex vivo.

Our results of the ROC curve analyses for differentiating between metastatic and non-metastatic lymph nodes in patients with oral carcinoma demonstrated that the AUCs for D values and K values were significantly greater than the AUC for ADC values. Furthermore, the cut-off D value and the cut-off K value were found to be useful for differentiating metastatic from non-metastatic lymph nodes in patients with oral carcinoma.

There were two limitations to our study. First, the patient population (n = 27) is quite small and especially the population of Grade 3 carcinoma is extremely small (n = 3) in order to define differences in imaging parameters between three different histologic grades. Nevertheless, after we corrected for multiple comparisons in the statistical analysis, we were able to obtain significant thresholds in order to differentiate between the different histologic grades. We believe that these findings need further confirming in a larger study including more patients with oral carcinoma.

Second, the number of b values (0, 500, 1000, and 2000 s/mm^2) used for estimating the DKI parameters was relatively small, compared with that used in the previous reports. This may have affected the curve fitting of the DKI data; nevertheless, the calculated DKI parameters were compatible with those in the previous reports [12,13]. Our ultimate goal would be the routine application of DKI as a noninvasive quantitative tool for accurate preoperative evaluation and selection of the optimal therapy for patients with oral carcinoma.

In conclusion, the D and K values derived from DKI were significantly

correlated with the histologic grades of oral carcinomas and showed significant differences between metastatic and non-metastatic lymph nodes in patients with coral carcinoma. Therefore, our results have demonstrated that DKI has the potential to provide useful information for evaluating the histologic grade and lymph node metastasis in patients with oral carcinoma.

References

[1] Amin MB, Edge SB, Greene FL, Byrd DR, Brookland RK, Washington MK, et al. AJCC cancer staging manual. 8th ed. New York: Springer; 2017, p. 79-94.

[2] Arora A, Husain N, Bansal A, Neyaz A, Jaiswal R, Jain K, et al. Development of a New Outcome Prediction Model in Early-stage Squamous Cell Carcinoma of the Oral Cavity Based on Histopathologic Parameters With Multivariate Analysis: The Aditi-Nuzhat Lymph-node Prediction Score (ANLPS) System. Am J Surg Pathol 2017;41:950-60.

[3] Hasegawa T, Tanakura M, Takeda D, Sakakibara A, Akashi M, Minamikawa T, et al. Risk factors associated with distant metastasis in patients with oral squamous cell carcinoma. Otolaryngol Head Neck Surg 2015;152:1053-60.

[4] Kahling C, Langguth T, Roller F, Kroll T, Krombach G, Knitschke M, et al. A retrospective analysis of preoperative staging modalities for oral squamous cell carcinoma. J Craniomaxillofac Surg 2016;44:1952-6.

[5] Kreppel M, Nazarli P, Grandoch A, Safi AF, Zirk M, Nickenig HJ, et al. Clinical and histopathological staging in oral squamous cell carcinoma - Comparison of the prognostic significance. Oral Oncol 2016;60:68-73.

[6] Angelelli G, Moschetta M, Limongelli L, Albergo A, Lacalendola E, Brindicci F, et al. Endocavitary sonography of early oral cavity malignant tumors. Head Neck 2017;39:1349-56.

[7] Rollon-Mayordomo A, Creo-Martinez T, Marin-Lapeira Y, Rodriguez-Ruiz JA, Infante-Cossio P. Preoperative ultrasonography for evaluation of clinically N0 neck in oral cavity carcinoma. J Craniomaxillofac Surg 2017;45:420-6.

[8] Alsaffar HA, Goldstein DP, King EV, de Almeida JR, Brown DH, Gilbert RW, et al. Correlation between clinical and MRI assessment of depth of invasion in oral tongue squamous cell carcinoma. J Otolaryngol Head Neck Surg 2016;45:61.

[9] Singh A, Thukral CL, Gupta K, Sood AS, Singla H, Singh K. Role of MRI in Evaluation of Malignant Lesions of Tongue and Oral Cavity. Pol J Radiol 2017;82:92-9.

[10] Raab P, Hattingen E, Franz K, Zanella FE, Lanfermann H. Cerebral gliomas: diffusional kurtosis imaging analysis of microstructural differences. Radiology 2010;254:876-81.

[11] Van Cauter S, Veraart J, Sijbers J, Peeters RR, Himmelreich U, De Keyzer F, et

al. Gliomas: diffusion kurtosis MR imaging in grading. Radiology 2012;263:492-501.
[12] Rosenkrantz AB, Sigmund EE, Johnson G, Babb JS, Mussi TC, Melamed J, et al. Prostate cancer: feasibility and preliminary experience of a diffusional kurtosis model for detection and assessment of aggressiveness of peripheral zone cancer. Radiology 2012;264:126-35.
[13] Rosenkrantz AB, Padhani AR, Chenevert TL, Koh DM, De Keyzer F, Taouli B, et al. Body diffusion kurtosis imaging: Basic principles, applications, and considerations for clinical practice. J Magn Reson Imaging 2015;42:1190-202.
[14] Sun K, Chen X, Chai W, Fei X, Fu C, Yan X, et al. Breast Cancer: Diffusion Kurtosis MR Imaging-Diagnostic Accuracy and Correlation with Clinical-Pathologic Factors. Radiology 2015;277:46-55.
[15] Yamada I, Hikishima K, Miyasaka N, Tokairin Y, Ito E, Kawano T, et al. Esophageal carcinoma: Evaluation with q-space diffusion-weighted MR imaging ex vivo. Magn Reson Med 2015;73:2262-73.
[16] Yamada I, Hikishima K, Miyasaka N, Kato K, Ito E, Kojima K, et al. q-space MR imaging of gastric carcinoma ex vivo: Correlation with histopathologic findings. Magn Reson Med 2016;76:602-12.
[17] Jensen JH, Helpern JA, Ramani A, Lu H, Kaczynski K. Diffusional kurtosis imaging: the quantification of non-gaussian water diffusion by means of magnetic resonance imaging. Magn Reson Med 2005;53:1432-40.
[18] Jensen JH, Helpern JA. MRI quantification of non-Gaussian water diffusion by kurtosis analysis. NMR Biomed 2010;23:698-710.
[19] Sakamoto J, Kuribayashi A, Kotaki S, Fujikura M, Nakamura S, Kurabayashi T. Application of diffusion kurtosis imaging to odontogenic lesions: Analysis of the cystic component. J Magn Reson Imaging 2016;44:1565-71.
[20] Sugahara T, Korogi Y, Kochi M, Ikushima I, Shigematu Y, Hirai T, et al. Usefulness of diffusion-weighted MRI with echo-planar technique in the evaluation of cellularity in gliomas. J Magn Reson Imaging 1999;9:53-60.
[21] Kono K, Inoue Y, Nakayama K, Shakudo M, Morino M, Ohata K, et al. The role of diffusion-weighted imaging in patients with brain tumors. AJNR Am J Neuroradiol 2001;22:1081-8.
[22] Koral K, Mathis D, Gimi B, Gargan L, Weprin B, Bowers DC, et al. Common pediatric cerebellar tumors: correlation between cell densities and apparent diffusion coefficient metrics. Radiology 2013;268:532-7.

[23] Sumi M, Sakihama N, Sumi T, Morikawa M, Uetani M, Kabasawa H, et al. Discrimination of metastatic cervical lymph nodes with diffusion-weighted MR imaging in patients with head and neck cancer. AJNR Am J Neuroradiol 2003;24:1627-34.
[24] King AD, Ahuja AT, Yeung DK, Fong DK, Lee YY, Lei KI, et al. Malignant cervical lymphadenopathy: diagnostic accuracy of diffusion-weighted MR imaging. Radiology 2007;245:806-13.
[25] Vandecaveye V, De Keyzer F, Vander Poorten V, Dirix P, Verbeken E, Nuyts S, et al. Head and neck squamous cell carcinoma: value of diffusion-weighted MR imaging for nodal staging. Radiology 2009;251:134-46.
[26] Wu LM, Xu JR, Hua J, Gu HY, Zhu J, Hu J. Value of diffusion-weighted MR imaging performed with quantitative apparent diffusion coefficient values for cervical lymphadenopathy. J Magn Reson Imaging 2013;38:663-70.

Table 1

D, K, and ADC values in the different histologic grades of oral carcinomas.

Histologic Grades	D Values ($\times 10^{-3}$ mm^2/s)	K Values (a.u.)	ADC Values ($\times 10^{-3}$ mm^2/s)
Grade 1 (n = 13)	2.062 ± 0.231*	0.735 ± 0.061*	0.808 ± 0.064
Grade 2 (n = 11)	1.609 ± 0.133	0.858 ± 0.055	0.751 ± 0.057
Grade 3 (n = 3)	1.397 ± 0.053	1.027 ± 0.103	0.774 ± 0.134

Note: Grade 1 = Well-differentiated, Grade 2 = Moderately differentiated, Grade 3 = Poorly differentiated. a.u. = arbitrary units. * = Significantly different for the different histologic grades of the oral carcinomas ($P < 0.001$).

Table 2

D, K, and ADC values of the metastatic and non-metastatic lymph nodes in patients with oral carcinoma.

Lymph Nodes	D Values ($\times 10^{-3}$ mm^2/s)	K Values (a.u.)	ADC Values ($\times 10^{-3}$ mm^2/s)
Non-metastatic (n = 16)	2.054 ± 0.333*	0.775 ± 0.078*	0.771 ± 0.039
Metastatic (n = 11)	1.351 ± 0.285	1.079 ± 0.182	0.741 ± 0.054

Note: a.u. = arbitrary units. * = Significantly different between the metastatic and non-metastatic lymph nodes of the oral carcinomas ($P < 0.001$).

Table 3

ROC curve analyses of D, K, and ADC values for differentiating grade 2 or grade 3 from grade 1 oral carcinomas.

Parameter	AUC	Optimal Threshold	Sensitivity (%)	Specificity (%)	P Value
D values	0.989	≤ 1.881 ($\times 10^{-3}$ mm^2/s)	100.00 (14/14)	92.31 (12/13)	0.0115
K values	0.978	> 0.814 (a.u.)	85.71 (12/14)	100.00 (13/13)	0.0089
ADC values	0.714	≤ 0.749 ($\times 10^{-3}$ mm^2/s)	50.00 (7/14)	100.00 (13/13)	NA

Note: Optimal threshold of each parameter was determined to maximize average of sensitivity and specificity. Data in parentheses are numbers used to calculate percentages. P value represents differences in comparison with performance of ADC. AUC = area under the curve. a.u. = arbitrary units. NA = not available.

Table 4

ROC curve analyses of D, K, and ADC values for differentiating grade 3 from grade 1 or grade 2 oral carcinomas.

Parameter	AUC	Optimal Threshold	Sensitivity (%)	Specificity (%)	P Value
D values	0.986	≤ 1.457 ($\times 10^{-3}$ mm^2/s)	100.00 (3/3)	95.83 (23/24)	0.0968
K values	0.986	> 0.893 (a.u.)	100.00 (3/3)	95.83 (23/24)	0.1075
ADC values	0.514	< 0.781 ($\times 10^{-3}$ mm^2/s)	66.67 (2/3)	58.33 (14/24)	NA

Note: Optimal threshold of each parameter was determined to maximize average of sensitivity and specificity. Data in parentheses are numbers used to calculate percentages. P value represents differences in comparison with performance of ADC. AUC = area under the curve. a.u. = arbitrary units. NA = not available.

Table 5

ROC curve analyses of D, K, and ADC values for differentiating metastatic from non-metastatic lymph nodes in patients with oral carcinoma.

Parameter	AUC	Optimal Threshold	Sensitivity (%)	Specificity (%)	P Value
D values	0.938	≤ 1.419 ($\times 10^{-3}$ mm^2/s)	90.91 (10/11)	100.00 (16/16)	0.0132
K values	0.977	> 0.834 (a.u.)	100.00 (11/11)	87.50 (14/16)	0.0077
ADC values	0.688	≤ 0.748 ($\times 10^{-3}$ mm^2/s)	54.55 (6/11)	81.25 (13/16)	NA

Note: Optimal threshold of each parameter was determined to maximize average of sensitivity and specificity. Data in parentheses are numbers used to calculate percentages. P value represents differences in comparison with performance of ADC. AUC = area under the curve. a.u. = arbitrary units. NA = not available.

CAPTIONS FOR ILLUSTRATIONS

Figure 1. Box plots of the DKI parameters in the different histologic grades of oral carcinomas.
(a) Comparison of the D values in the different histologic grades of oral carcinomas showing a significant inverse correlation ($r = -0.885$; $P < 0.001$).
(b) Comparison of the K values in the different histologic grades of oral carcinomas showing a significant positive correlation ($r = 0.869$; $P < 0.001$). (a.u. = arbitrary units.)
(c) Comparison of the ADC values in the different histologic grades of oral carcinomas showing no significant correlation ($r = -0.311$; $P = 0.115$).

Figure 2. Images of a 50-year-old man with Grade 1 oral carcinoma.
(a) T2-weighted image shows a hyperintense mass lesion (arrow) in the right tongue. A red ROI is placed on the mass lesion.
(b) D map shows that the mass lesion (arrow) is slightly hyperintense (D = 1.930 × 10^{-3} mm^2/s).
(c) K map shows that the mass lesion (arrow) is slightly hypointense (K = 0.717 a.u.).
(d) ADC map shows that the mass lesion (arrow) is hyperintense (ADC = 0.832 × 10^{-3} mm^2/s.
(e) Histopathologic examination shows well-differentiated squamous cell carcinoma (Grade 1). (Hematoxylin-eosin stain; original magnification, x200.)

Figure 3. Images of an 81-year-old woman with Grade 3 oral carcinoma.
(a) T2-weighted image shows a hyperintense mass lesion (arrow) in the left tongue. A red ROI is placed on the mass lesion.
(b) D map shows that the mass lesion (arrow) is slightly hypointense (D = 1.357 × 10^{-3} mm^2/s.
(c) K map shows that mass lesion (arrow) is slightly hyperintense (K = 1.053 a.u.).
(d) ADC map shows that the mass lesion (arrow) is hyperintense (ADC = 0.786 × 10^{-3} mm^2/s.
(e) Histopathologic examination shows poorly differentiated squamous cell carcinoma (Grade 3). (Hematoxylin-eosin stain; original magnification, x400.)

Figure 4. Box plots of the DKI parameters in non-metastatic and metastatic lymph nodes in patients with oral carcinoma.
(a) Comparison of the D values in non-metastatic and metastatic lymph nodes showing significant differences ($P < 0.001$).
(b) Comparison of the K values in non-metastatic and metastatic lymph nodes showing significant differences ($P < 0.001$).
(c) Comparison of the ADC values in non-metastatic and metastatic lymph nodes showing no significant differences ($P = 0.110$).

Figure 5. Images of a 50-year-old man with non-metastatic lymph nodes.
(a) T2-weighted image shows a swollen lymph node (arrow) in the right deep cervical region. A red ROI is placed on the lymph node.
(b) D map shows that the lymph node (arrow) is slightly hyperintense ($D = 1.926 \times 10^{-3}$ mm^2/s).
(c) K map shows that the lymph node (arrow) is slightly hypointense ($K = 0.727$ a.u.).
(d) ADC map shows that the lymph node (arrow) is hyperintense ($ADC = 0.782 \times 10^{-3}$ mm^2/s.
(e) Histopathologic examination shows that the lymph node does not have metastasis, but reactive hyperplasia. (Hematoxylin-eosin stain; original magnification, x10.)

Figure 6. Images of a 66-year-old man with metastatic lymph nodes.
(a) T2-weighted image shows an oval-shaped lymph node (arrow) in the left deep cervical region. A red ROI is placed on the lymph node.
(b) D map shows that the lymph node (arrow) is slightly hypointense ($D = 1.250 \times 10^{-3}$ mm^2/s.
(c) K map shows that the lymph node (arrow) is slightly hyperintense ($K = 1.126$ a.u.).
(d) ADC map shows that the lymph node (arrow) is hyperintense ($ADC = 0.733 \times 10^{-3}$ mm^2/s).
(e) Histopathologic examination shows that the lymph has metastasis of squamous cell carcinoma. (Hematoxylin-eosin stain; original magnification, x10.)

Figure 7. ROC curve analyses of the DKI parameters in patients with oral carcinoma.
(a) ROC curves for differentiating Grade 2 or Grade 3 from Grade 1 oral carcinomas.

The AUCs for D values (0.989; P = 0.0115) and K values (0.978; P = 0.0089) were significantly larger than the AUC for ADC values (0.714). There was no significant difference in the AUCs between the D values and K values (P = 0.6774).

(b) ROC curves for differentiating Grade 3 from Grade 1 or Grade 2 oral carcinomas. The AUCs for D values (0.986; P = 0.0968) and K values (0.986; P = 0.1075) were larger than the AUC for ADC values (0.514), although there was no significant difference).

(c) ROC curves for differentiating metastatic from non-metastatic lymph nodes in patients with oral carcinoma. The AUCs for the D values (0.938; P = 0.0132) and the K values (0.977; P = 0.0077) were significantly higher than the AUC for the ADC values (0.688). There was no significant difference in the AUCs between the D values and K values (P = 0.5249).

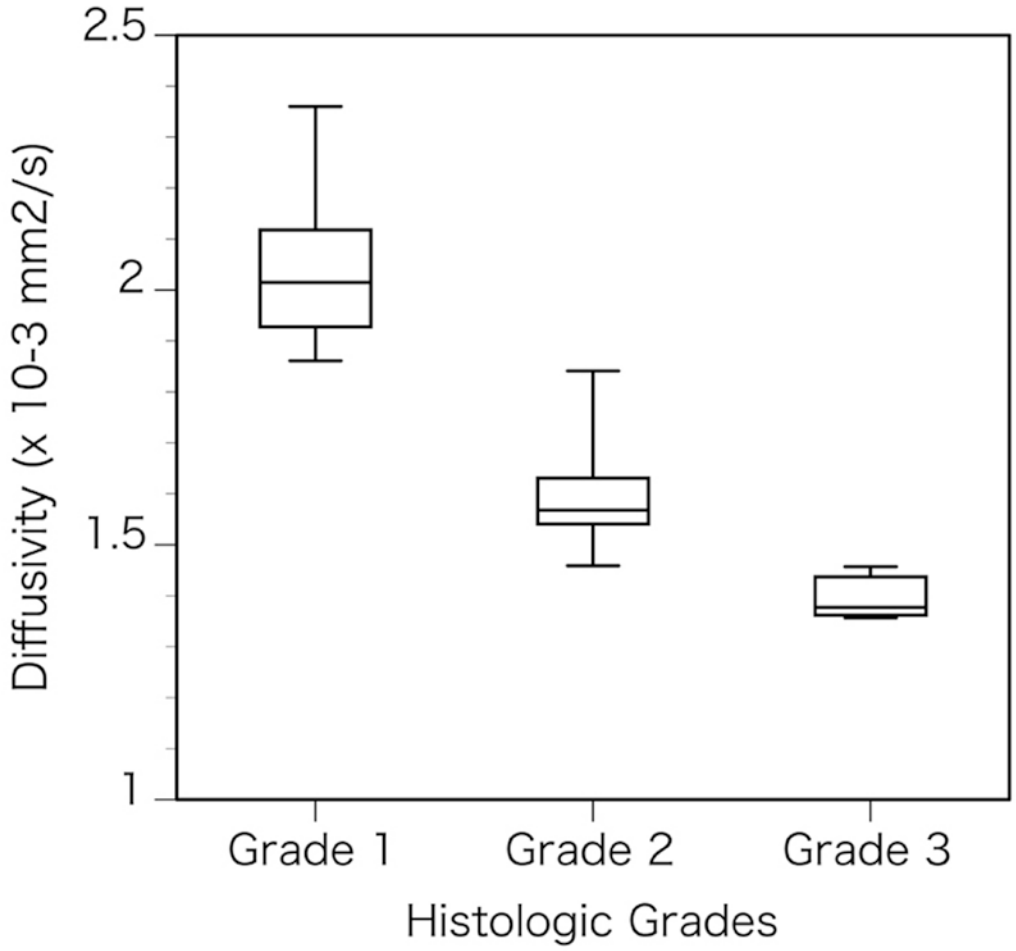

Figure 1. Box plots of the DKI parameters in the different histologic grades of oral carcinomas.

(a) Comparison of the D values in the different histologic grades of oral carcinomas showing a significant inverse correlation ($r = -0.885$; $P < 0.001$).

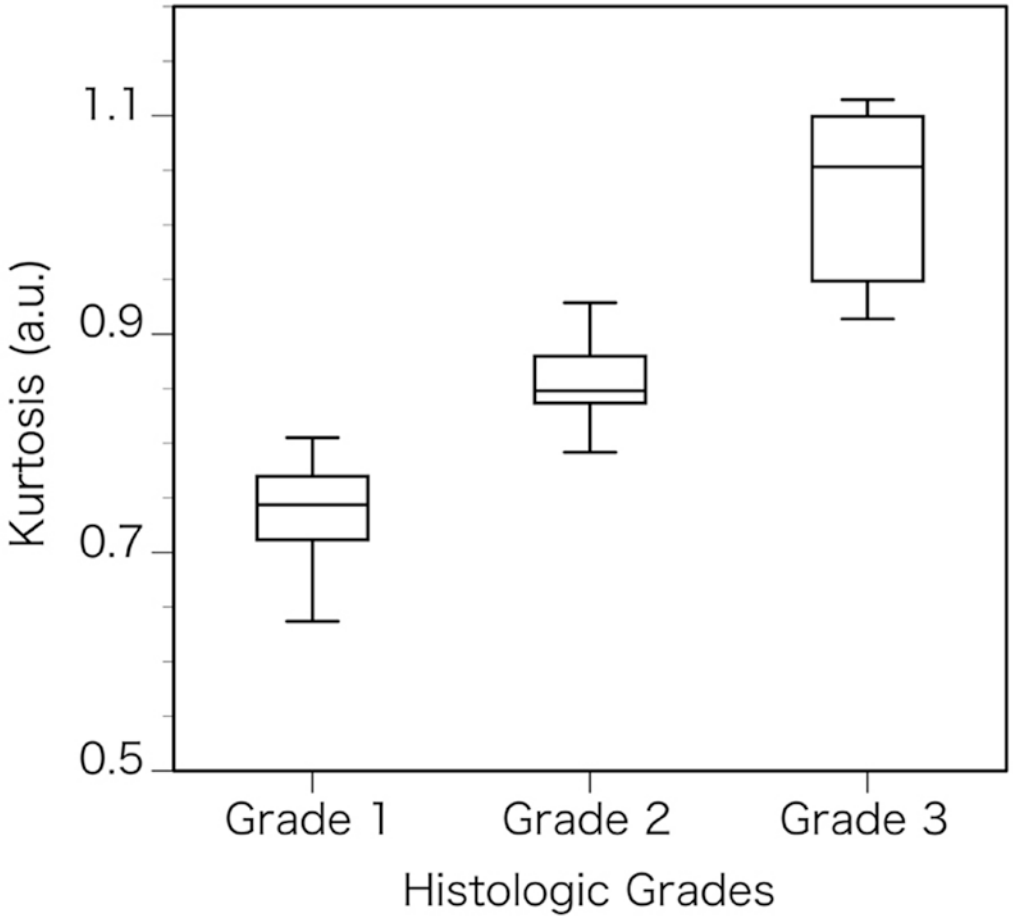

Figure 1. Box plots of the DKI parameters in the different histologic grades of oral carcinomas.

(b) Comparison of the K values in the different histologic grades of oral carcinomas showing a significant positive correlation ($r = 0.869$; $P < 0.001$). (a.u. = arbitrary units.)

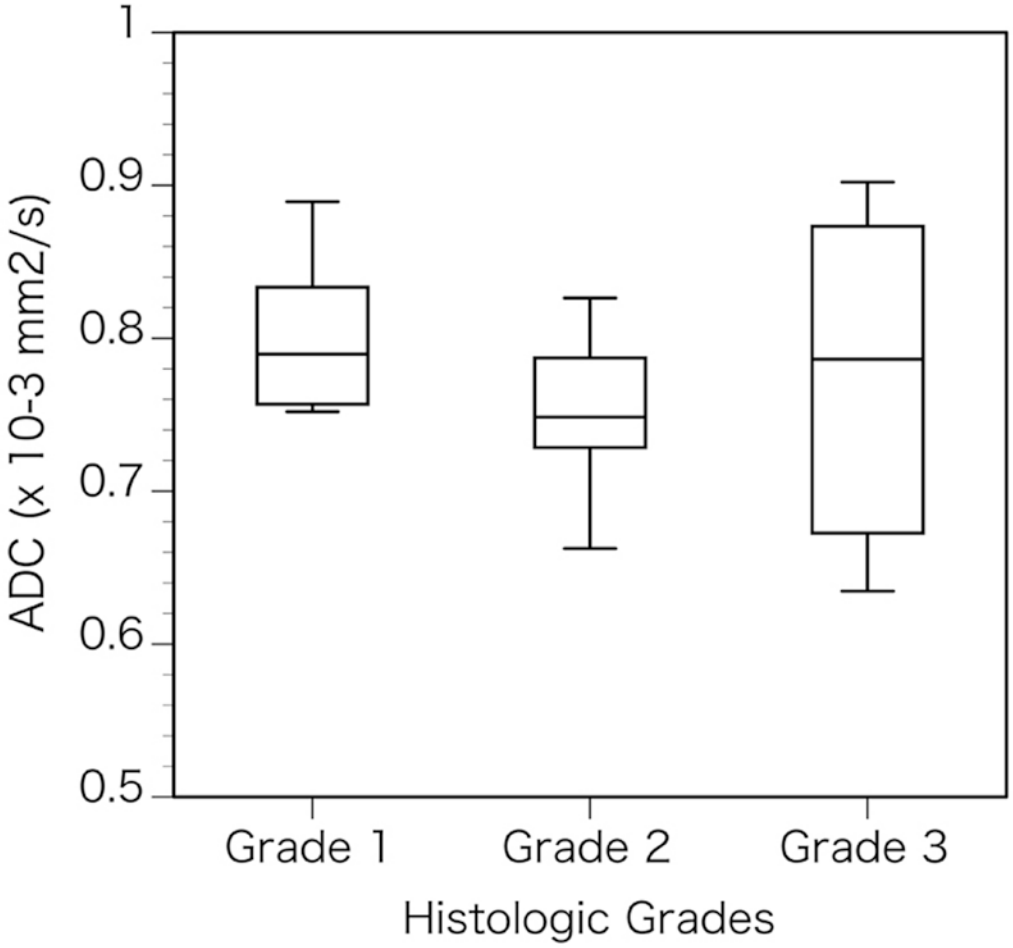

Figure 1. Box plots of the DKI parameters in the different histologic grades of oral carcinomas.

(c) Comparison of the ADC values in the different histologic grades of oral carcinomas showing no significant correlation (r = −0.311; P = 0.115).

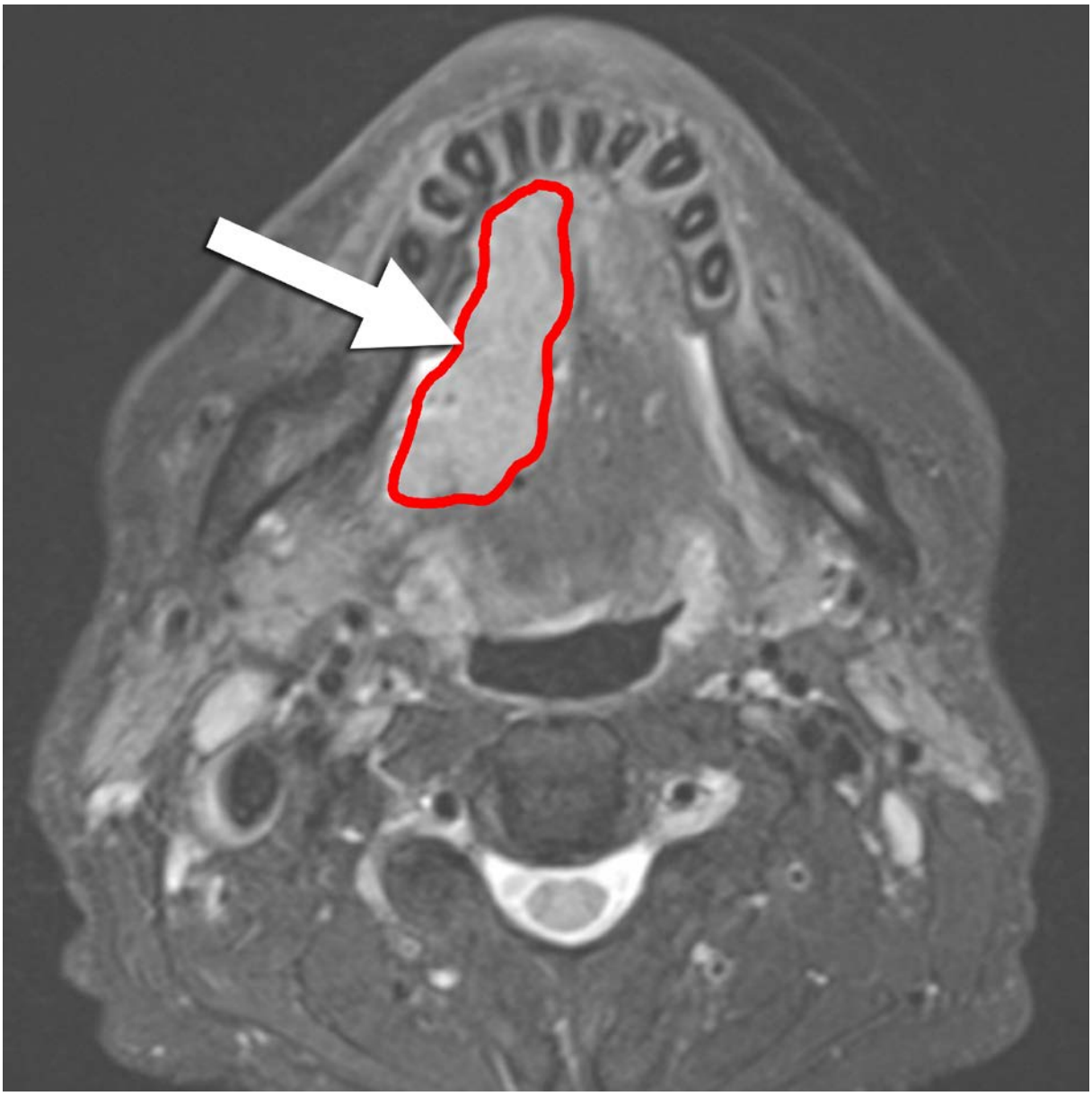

Figure 2. Images of a 50-year-old man with Grade 1 oral carcinoma.
(a) T2-weighted image shows a hyperintense mass lesion (arrow) in the right tongue. A red ROI is placed on the mass lesion.

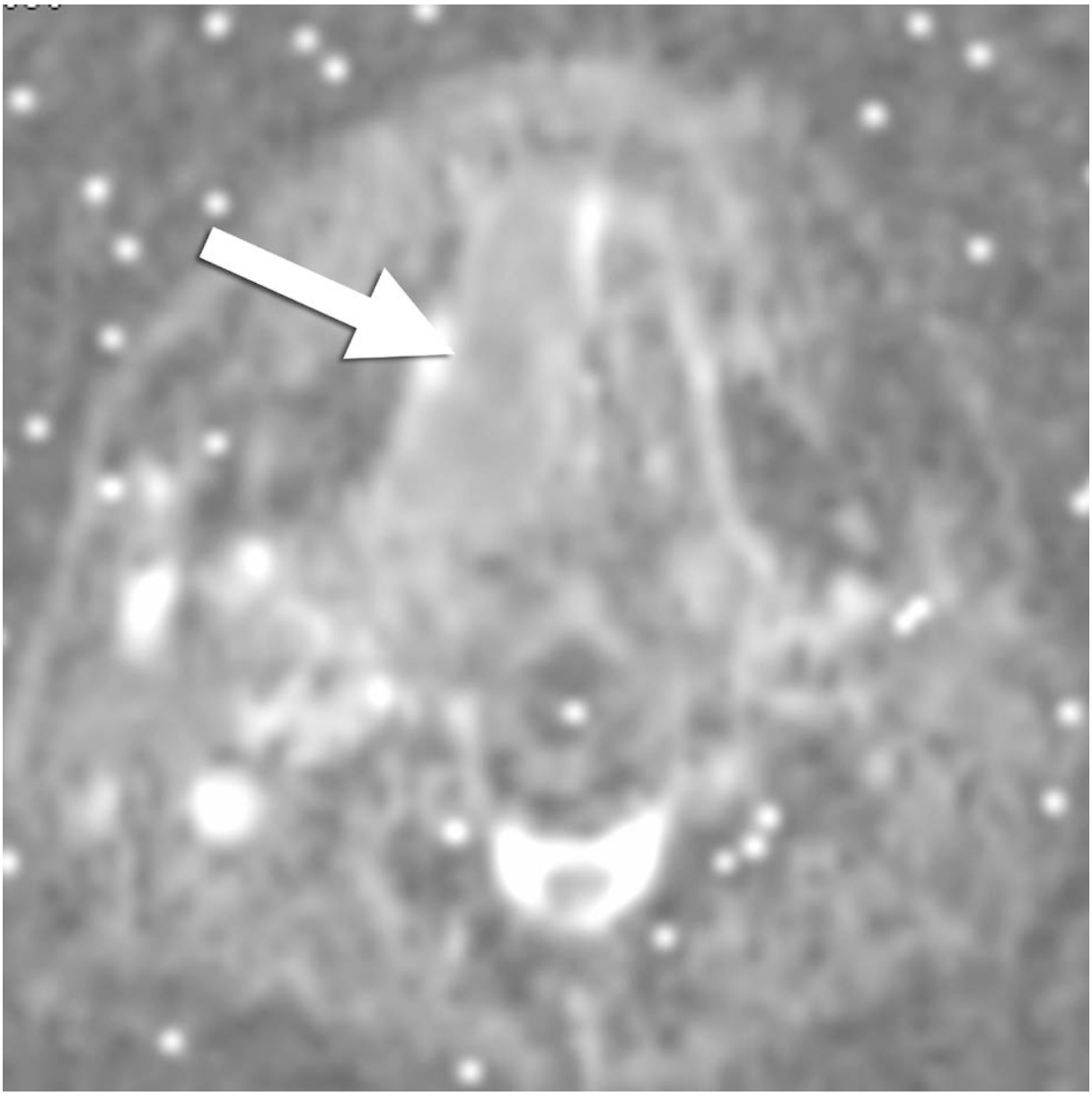

Figure 2. Images of a 50-year-old man with Grade 1 oral carcinoma.
(b) D map shows that the mass lesion (arrow) is slightly hyperintense (D = 1.930 × 10^{-3} mm^2/s).

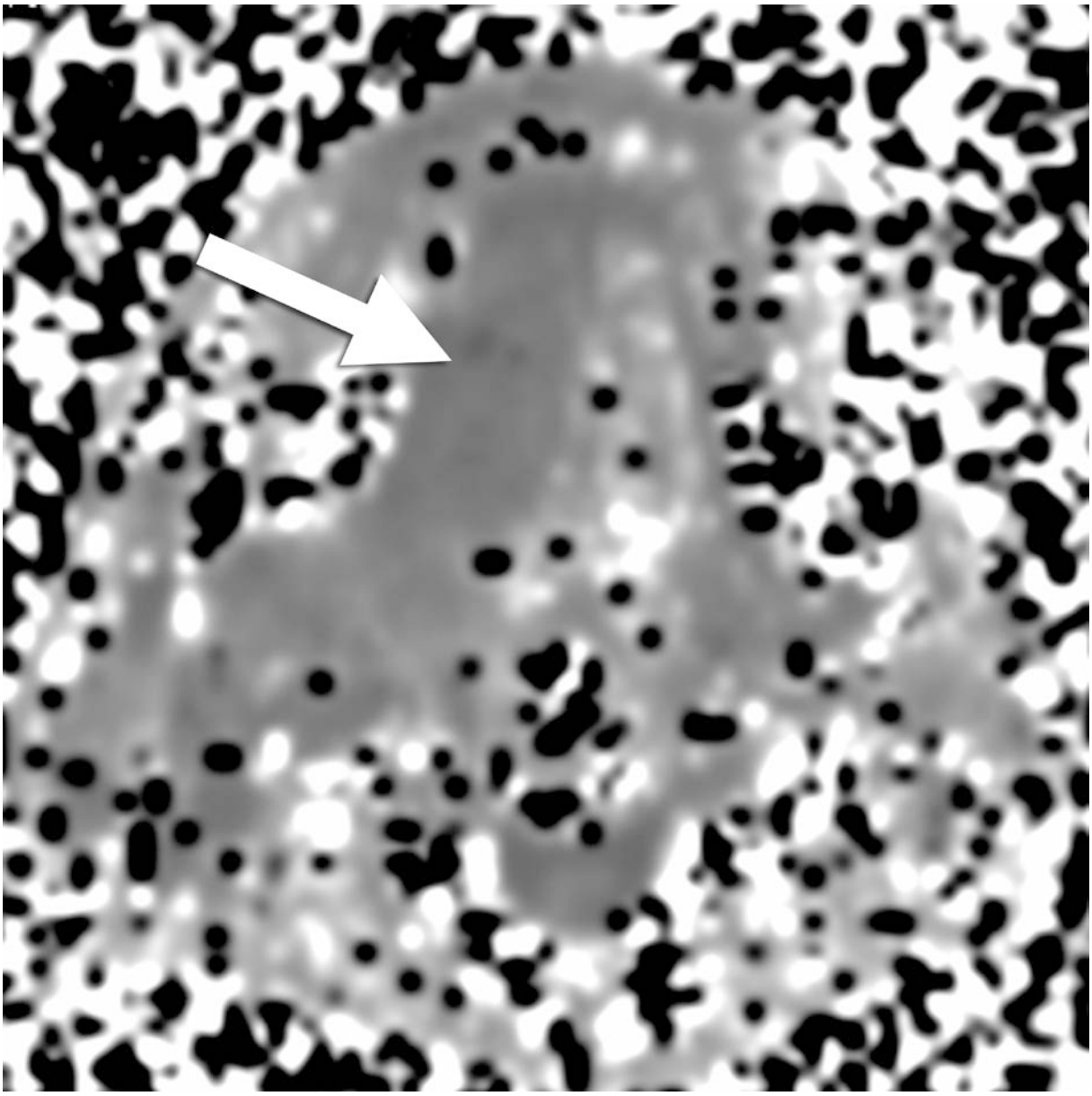

Figure 2. Images of a 50-year-old man with Grade 1 oral carcinoma.
(c) K map shows that the mass lesion (arrow) is slightly hypointense (K = 0.717 a.u.).

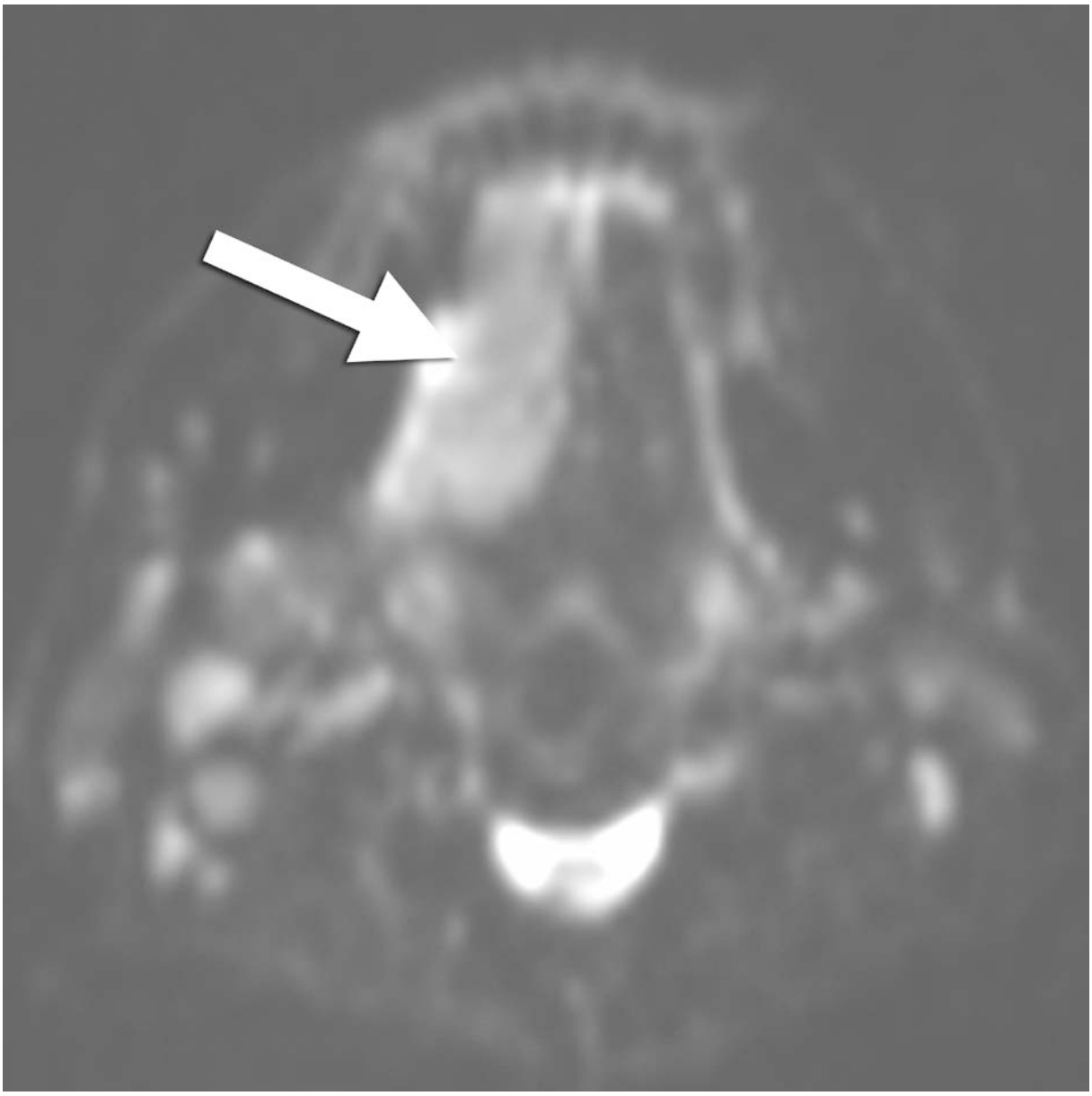

Figure 2. Images of a 50-year-old man with Grade 1 oral carcinoma.
(d) ADC map shows that the mass lesion (arrow) is hyperintense (ADC = 0.832 × 10^{-3} mm^2/s.

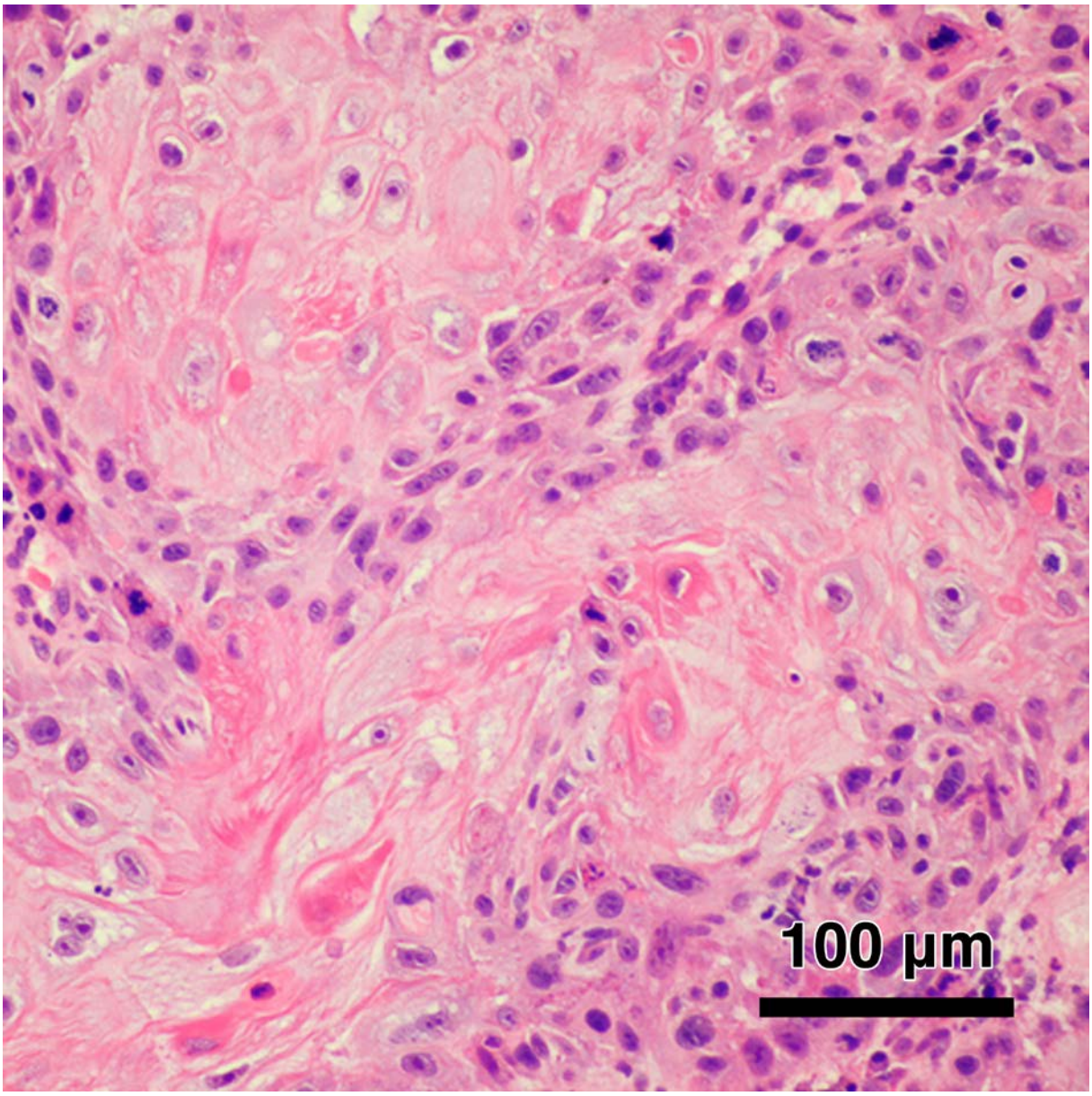

Figure 2. Images of a 50-year-old man with Grade 1 oral carcinoma.
(e) Histopathologic examination shows well-differentiated squamous cell carcinoma (Grade 1). (Hematoxylin-eosin stain; original magnification, x200.)

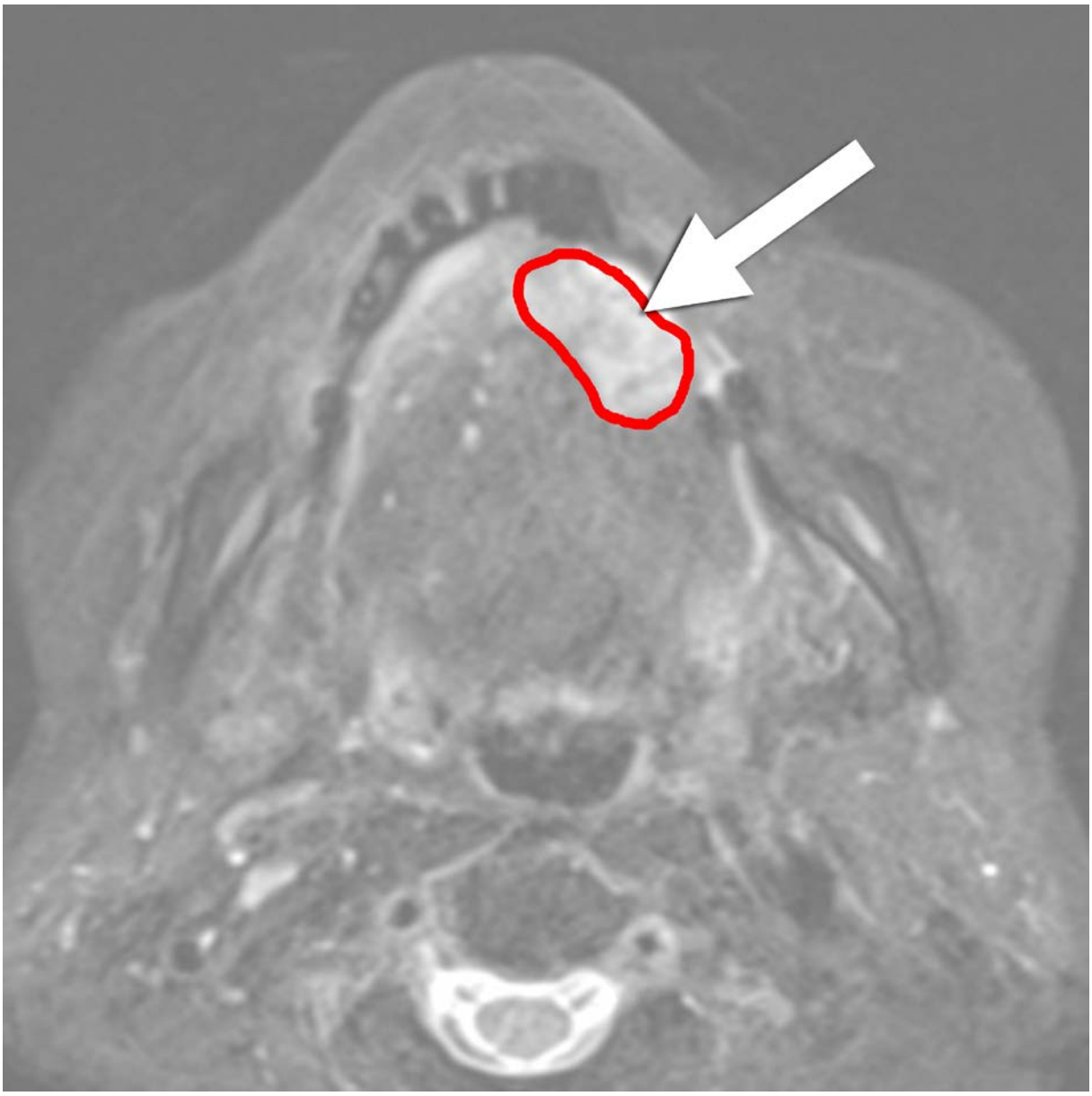

Figure 3. Images of an 81-year-old woman with Grade 3 oral carcinoma.
(a) T2-weighted image shows a hyperintense mass lesion (arrow) in the left tongue. A red ROI is placed on the mass lesion.

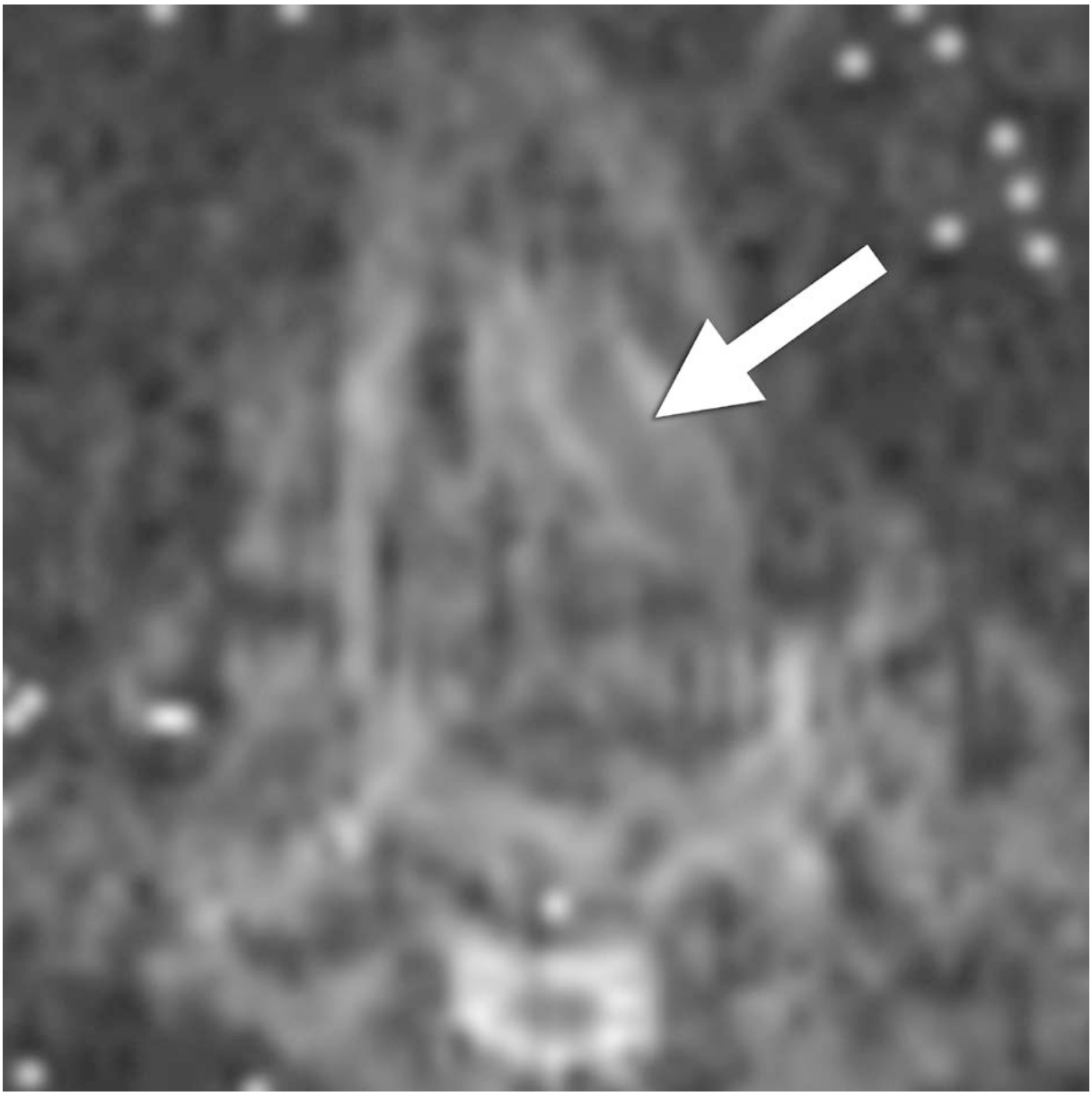

Figure 3. Images of an 81-year-old woman with Grade 3 oral carcinoma.
(b) D map shows that the mass lesion (arrow) is slightly hypointense (D = 1.357 × 10^{-3} mm^2/s.

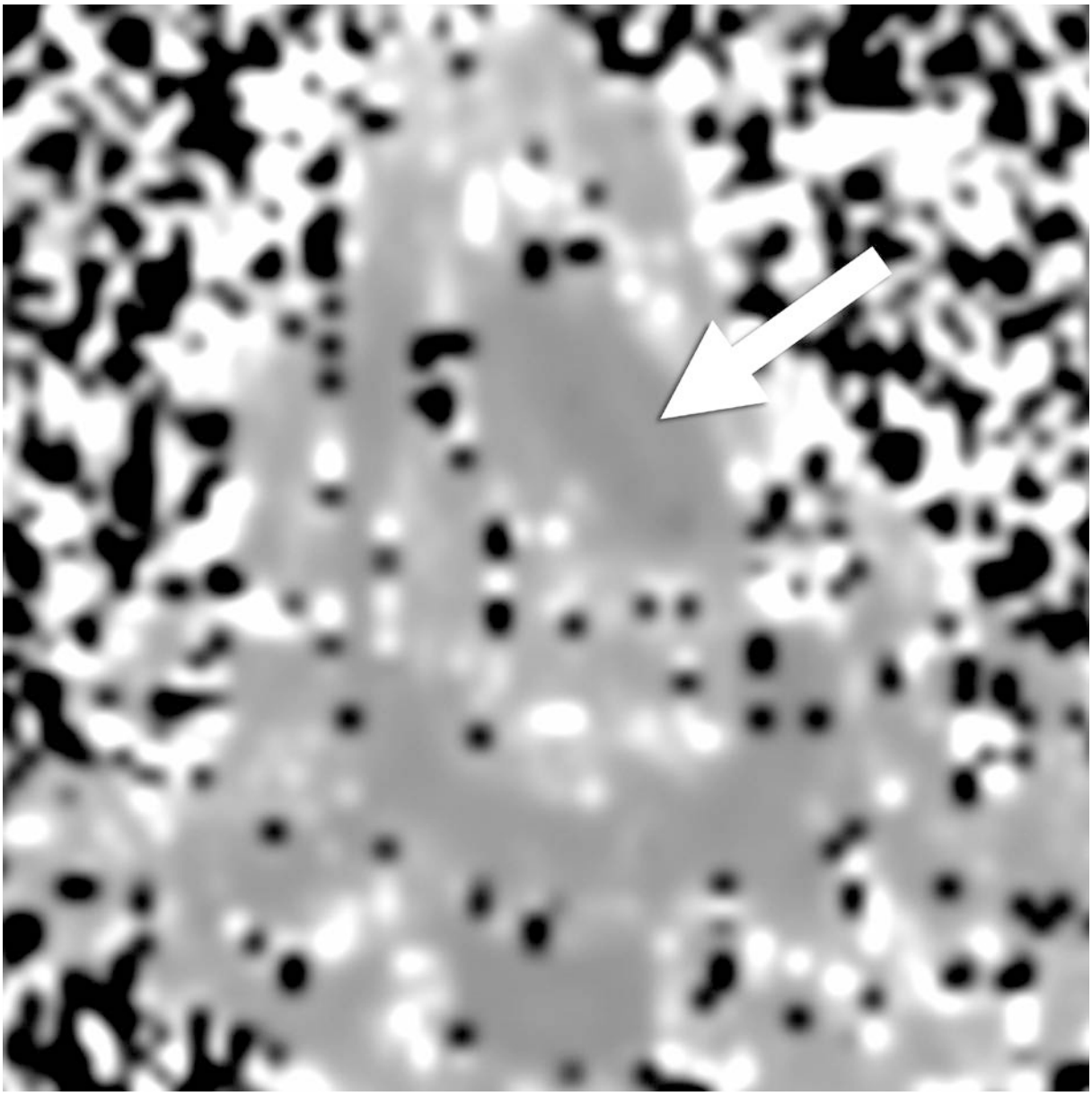

Figure 3. Images of an 81-year-old woman with Grade 3 oral carcinoma.
(c) K map shows that mass lesion (arrow) is slightly hyperintense (K = 1.053 a.u.).

Figure 3. Images of an 81-year-old woman with Grade 3 oral carcinoma.
(d) ADC map shows that the mass lesion (arrow) is hyperintense (ADC = 0.786 × 10^{-3} mm^2/s.

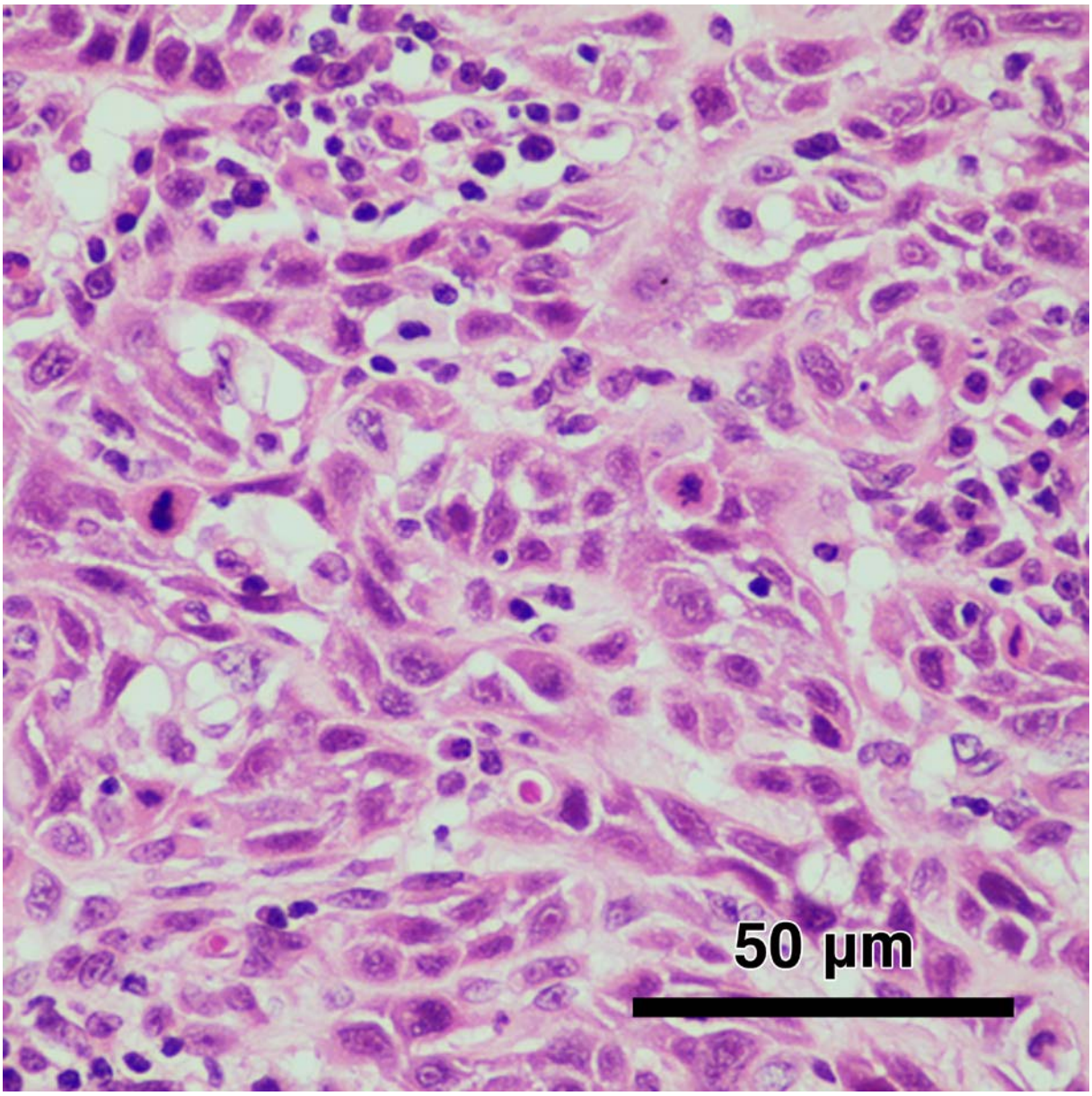

Figure 3. Images of an 81-year-old woman with Grade 3 oral carcinoma.
(e) Histopathologic examination shows poorly differentiated squamous cell carcinoma (Grade 3). (Hematoxylin-eosin stain; original magnification, x400.)

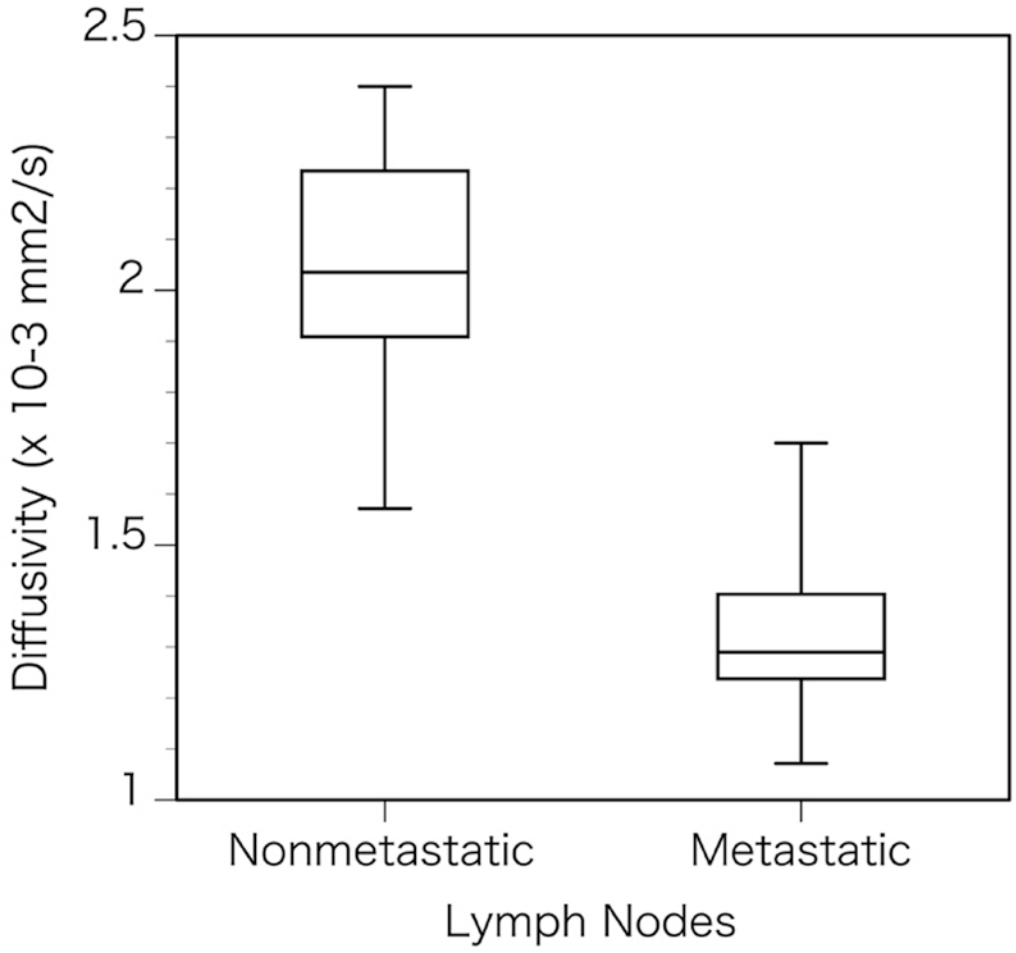

Figure 4. Box plots of the DKI parameters in non-metastatic and metastatic lymph nodes in patients with oral carcinoma.

(a) Comparison of the D values in non-metastatic and metastatic lymph nodes showing significant differences ($P < 0.001$).

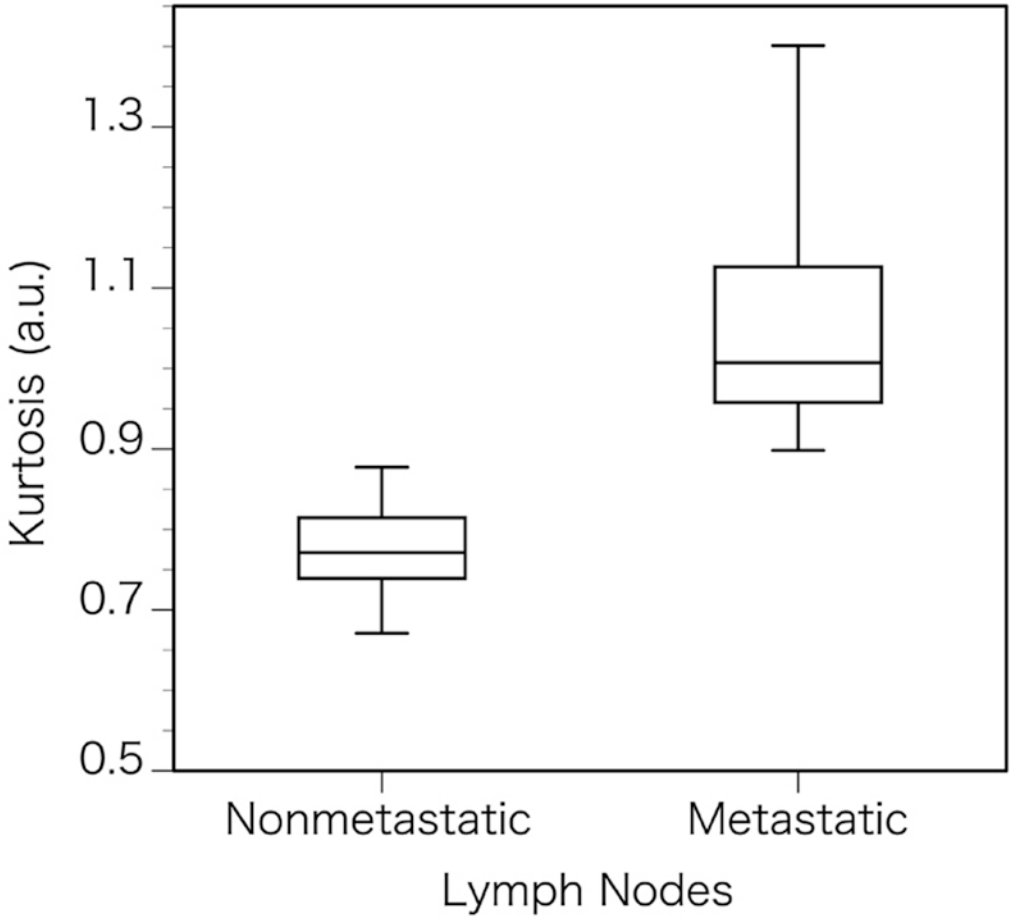

Figure 4. Box plots of the DKI parameters in non-metastatic and metastatic lymph nodes in patients with oral carcinoma.
(b) Comparison of the K values in non-metastatic and metastatic lymph nodes showing significant differences ($P < 0.001$).

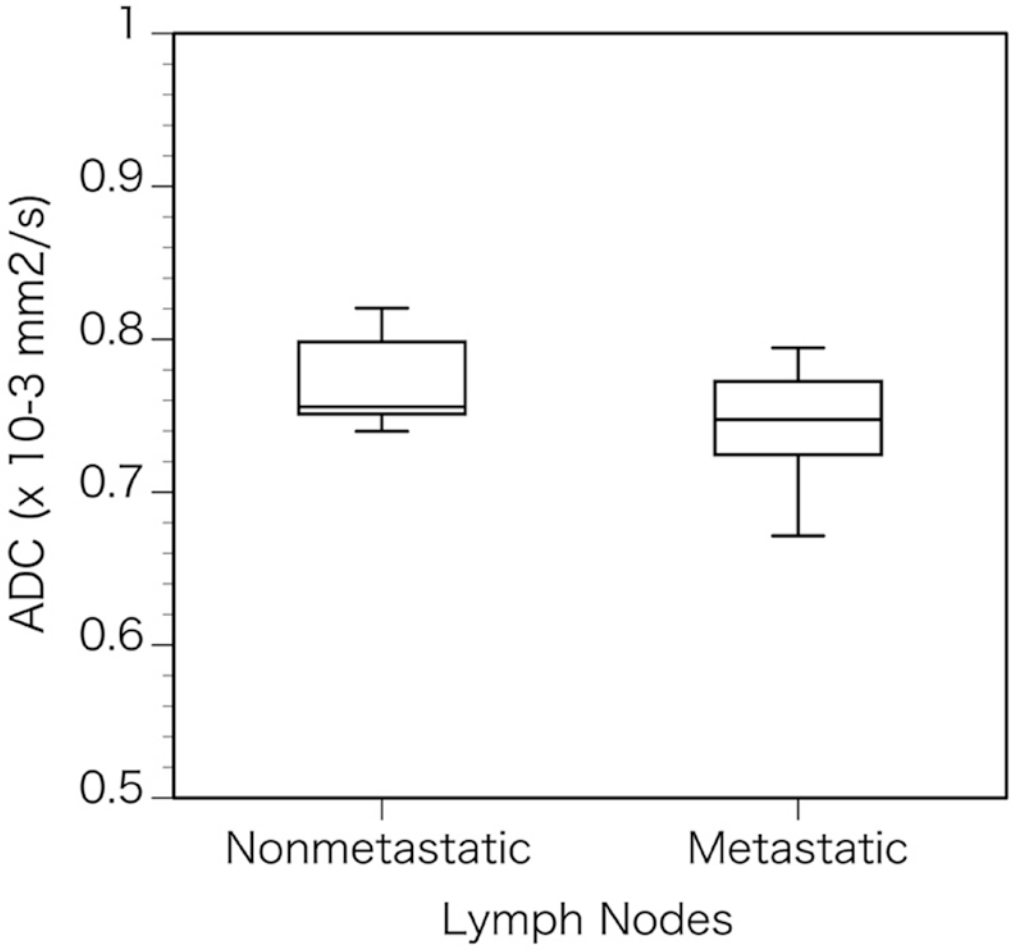

Figure 4. Box plots of the DKI parameters in non-metastatic and metastatic lymph nodes in patients with oral carcinoma.

(c) Comparison of the ADC values in non-metastatic and metastatic lymph nodes showing no significant differences (P = 0.110).

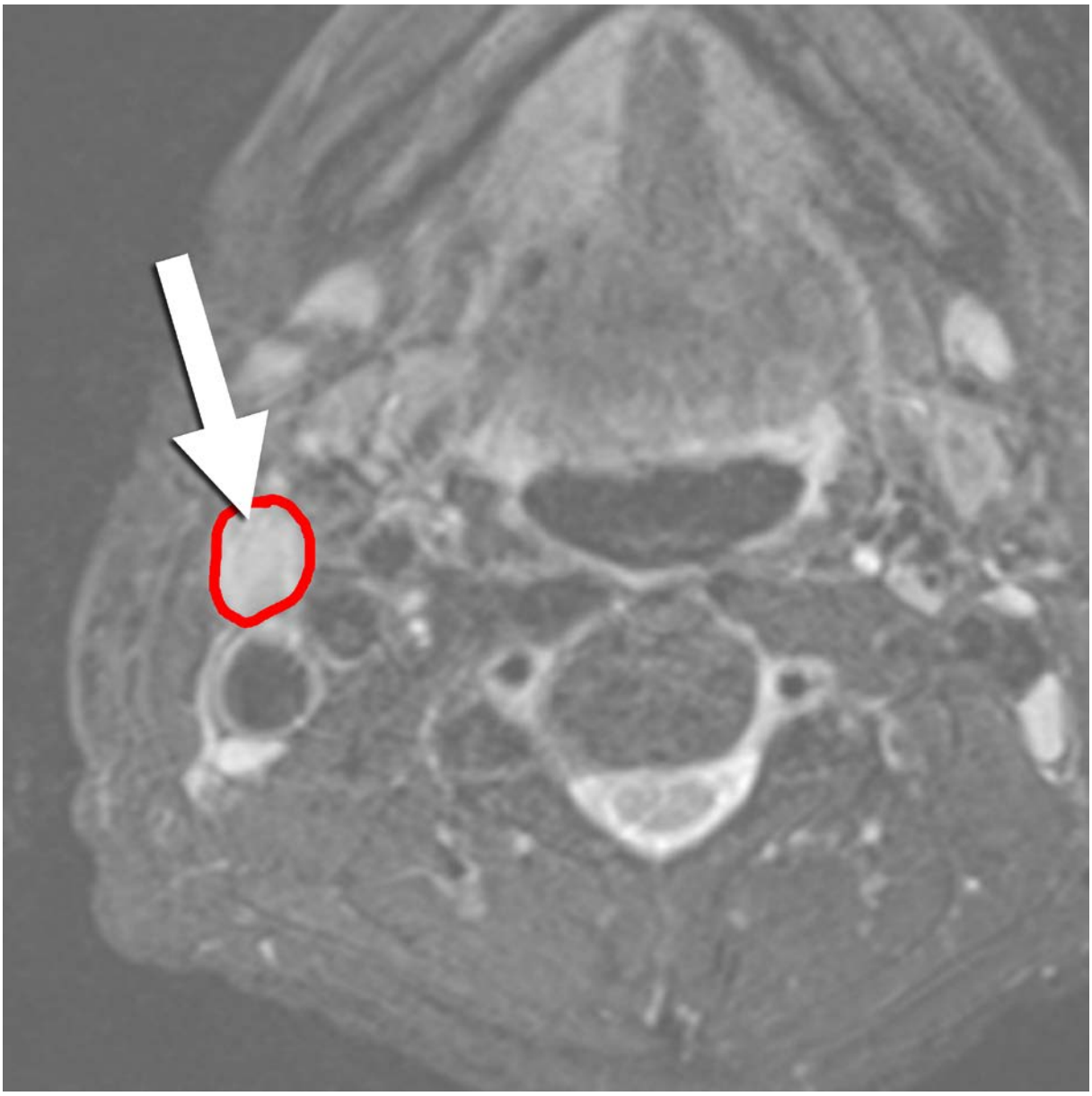

Figure 5. Images of a 50-year-old man with non-metastatic lymph nodes.
(a) T2-weighted image shows a swollen lymph node (arrow) in the right deep cervical region. A red ROI is placed on the lymph node.

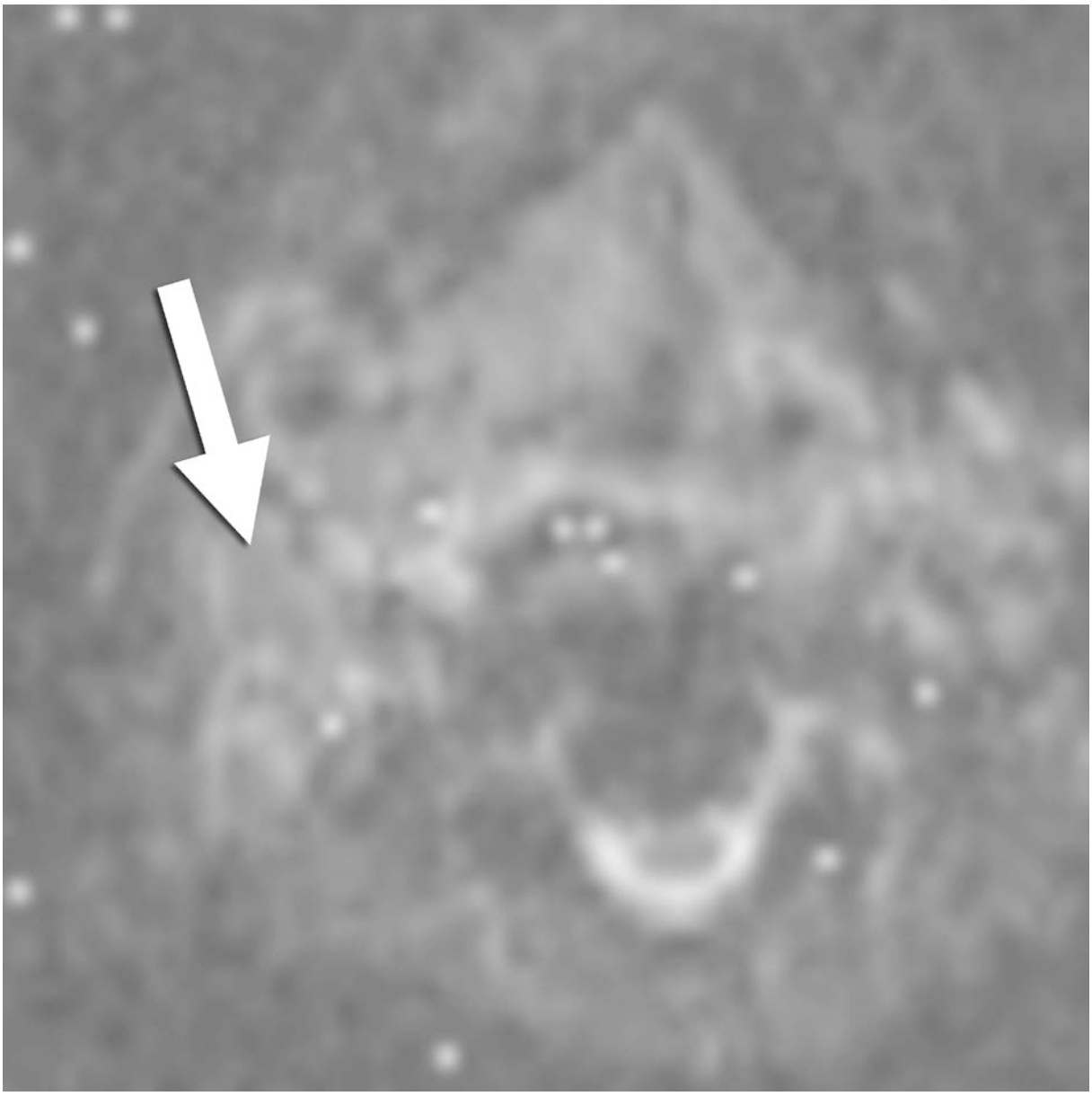

Figure 5. Images of a 50-year-old man with non-metastatic lymph nodes.
(b) D map shows that the lymph node (arrow) is slightly hyperintense (D = 1.926 × 10^{-3} mm^2/s).

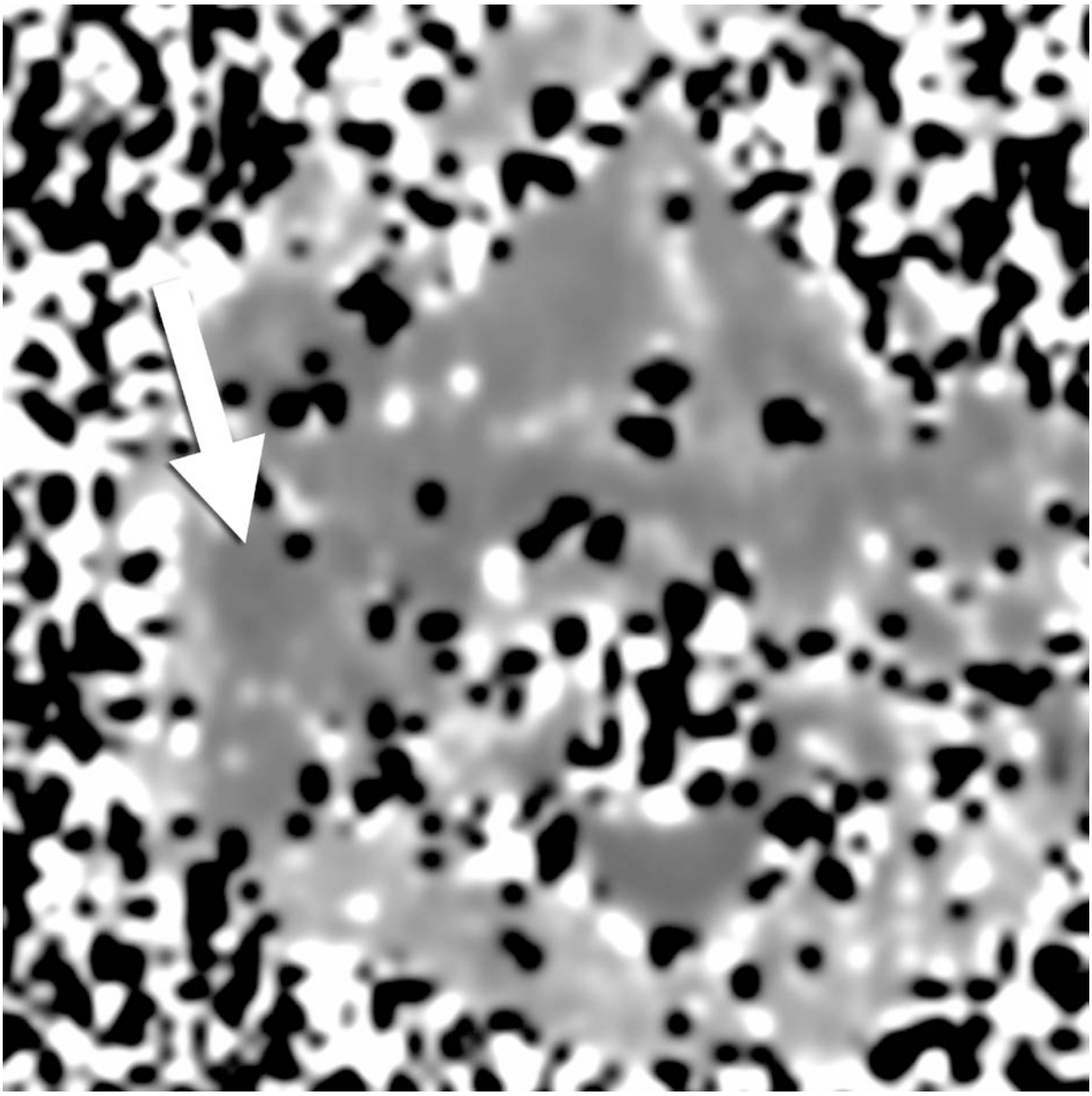

Figure 5. Images of a 50-year-old man with non-metastatic lymph nodes.
(c) K map shows that the lymph node (arrow) is slightly hypointense (K = 0.727 a.u.).

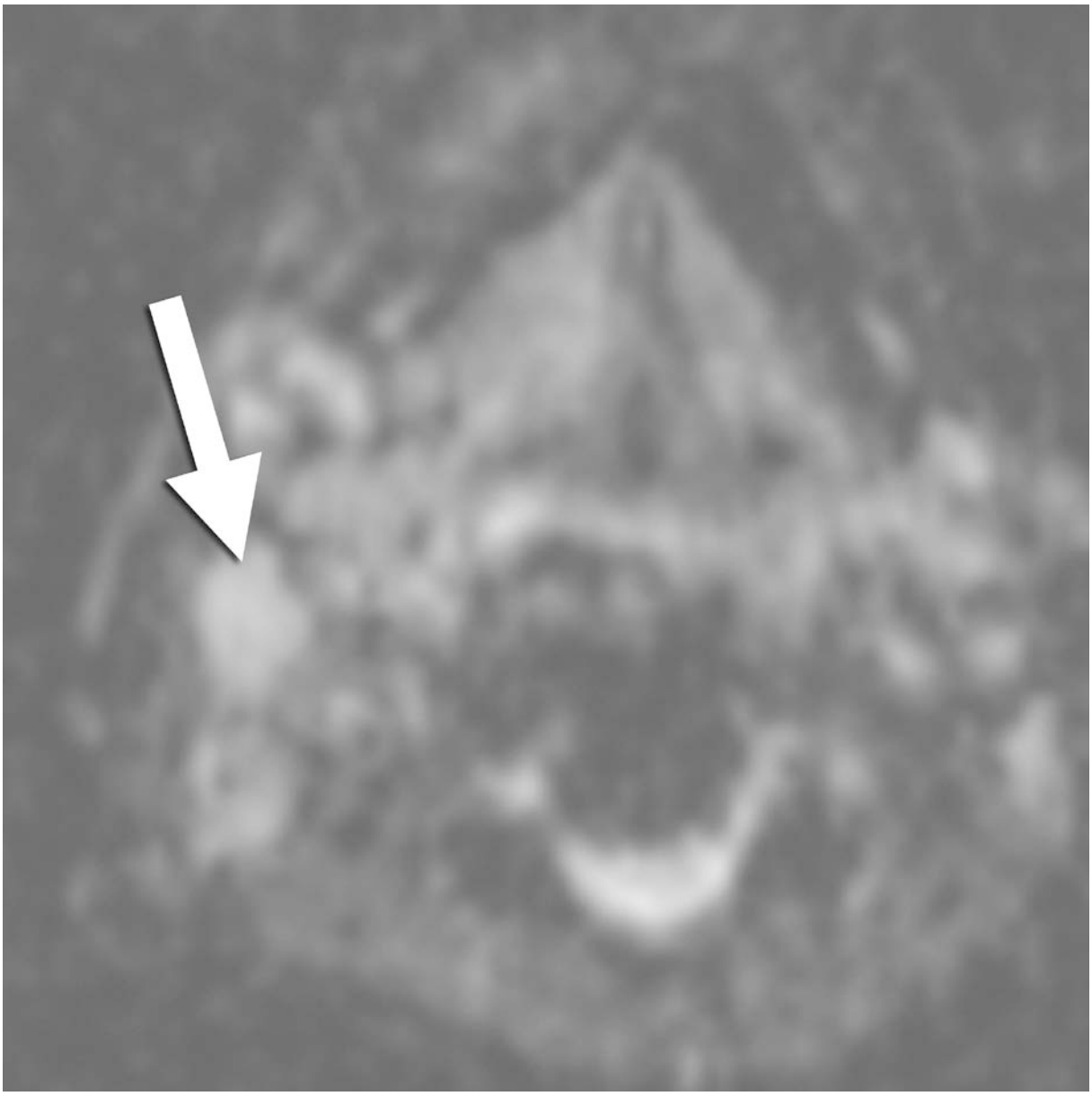

Figure 5. Images of a 50-year-old man with non-metastatic lymph nodes. **(d)** ADC map shows that the lymph node (arrow) is hyperintense (ADC = 0.782 × 10^{-3} mm^2/s.

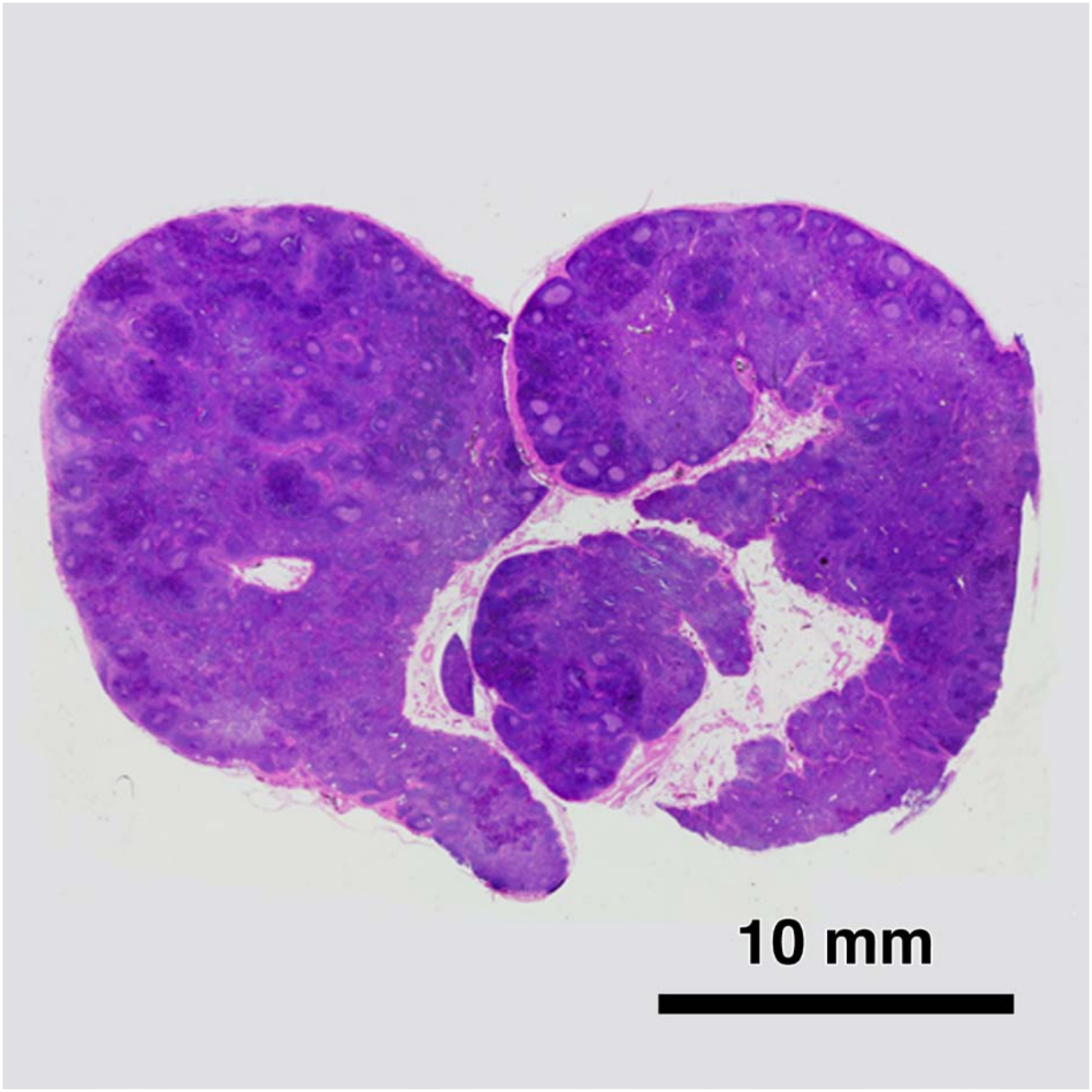

Figure 5. Images of a 50-year-old man with non-metastatic lymph nodes.
(e) Histopathologic examination shows that the lymph node does not have metastasis, but reactive hyperplasia. (Hematoxylin-eosin stain; original magnification, x10.)

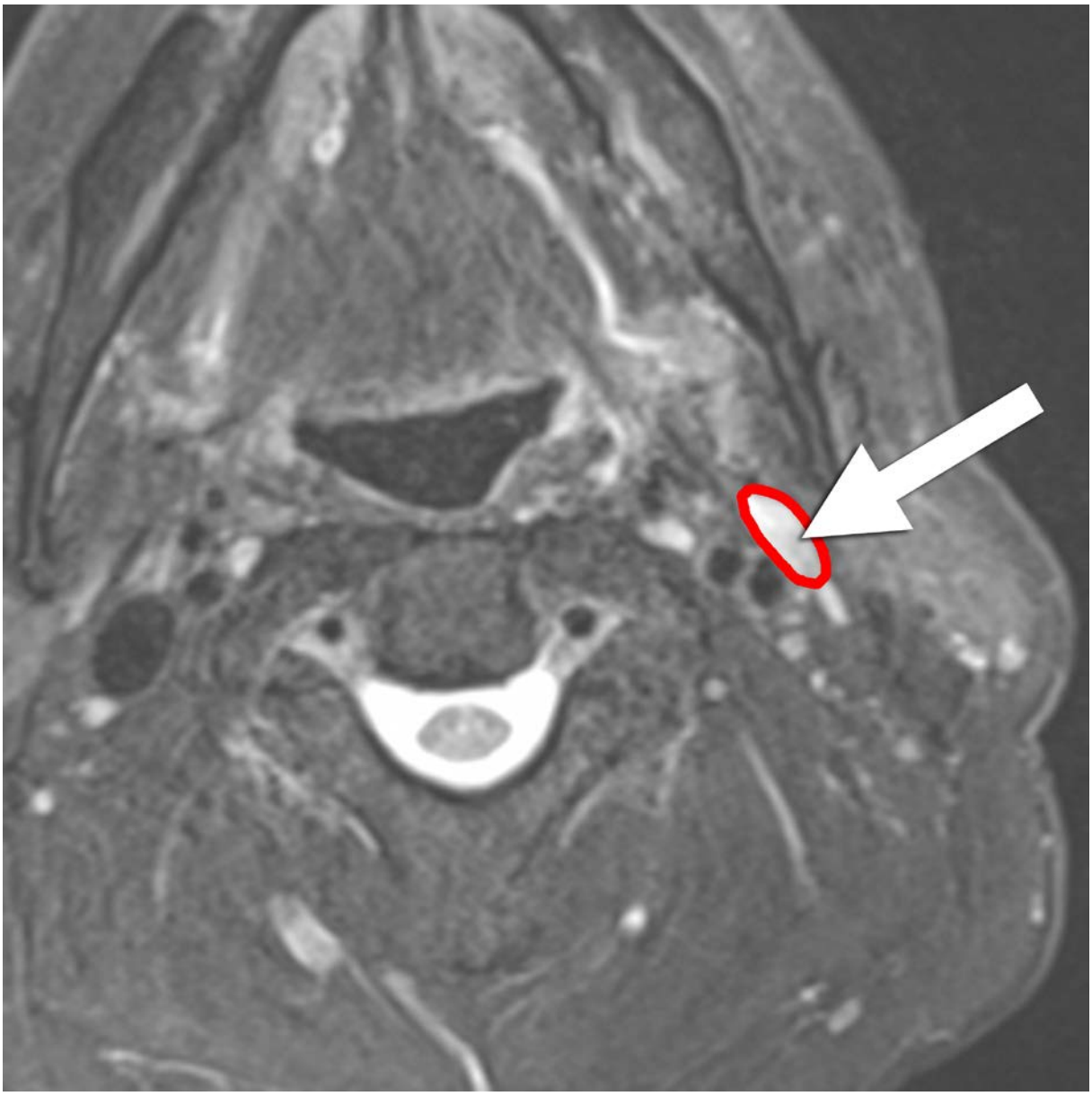

Figure 6. Images of a 66-year-old man with metastatic lymph nodes.
(a) T2-weighted image shows an oval-shaped lymph node (arrow) in the left deep cervical region. A red ROI is placed on the lymph node.

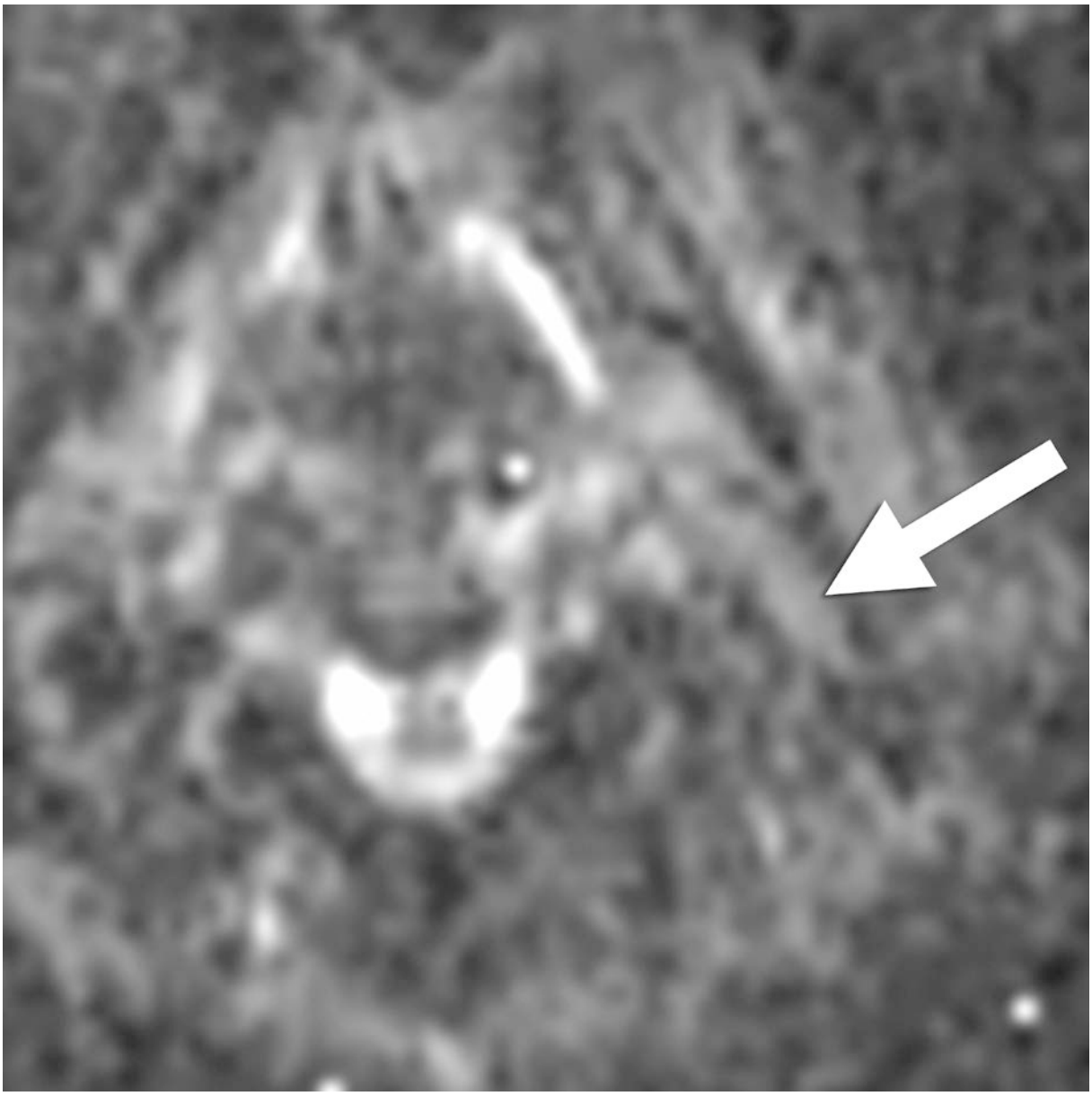

Figure 6. Images of a 66-year-old man with metastatic lymph nodes.
(b) D map shows that the lymph node (arrow) is slightly hypointense (D = 1.250 × 10^{-3} mm^2/s.

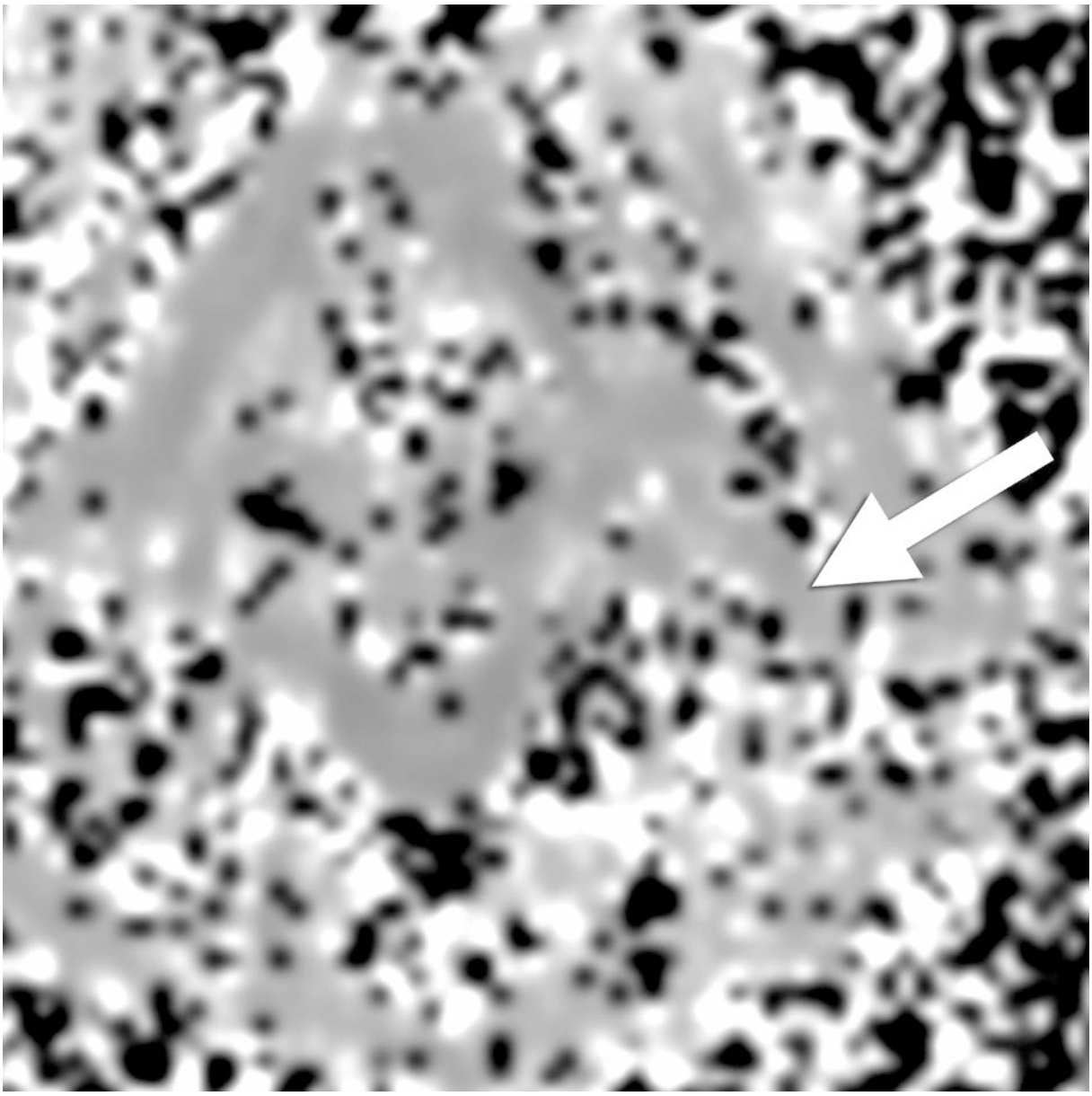

Figure 6. Images of a 66-year-old man with metastatic lymph nodes.
(c) K map shows that the lymph node (arrow) is slightly hyperintense (K = 1.126 a.u.).

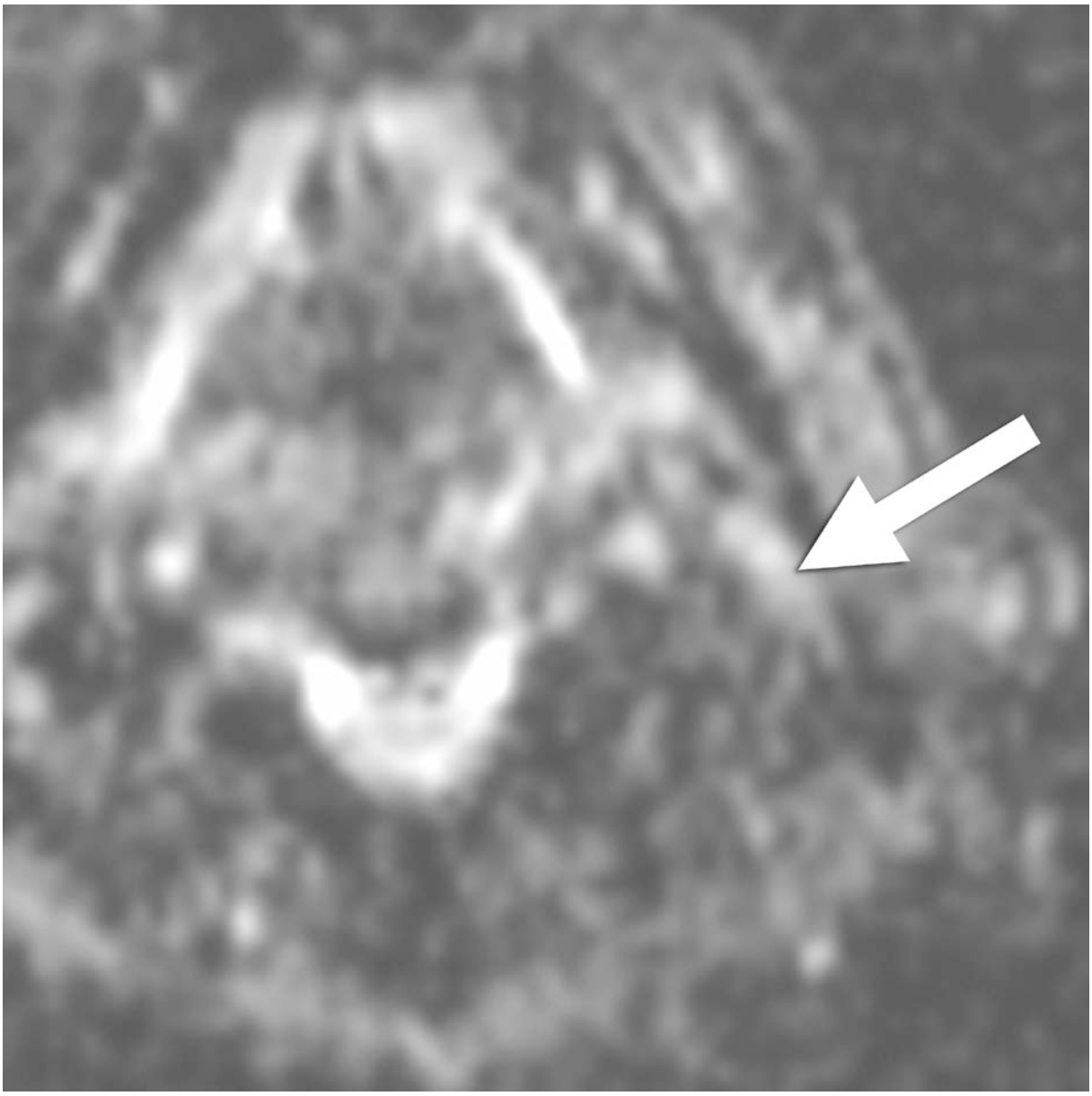

Figure 6. Images of a 66-year-old man with metastatic lymph nodes.
(d) ADC map shows that the lymph node (arrow) is hyperintense (ADC = 0.733 × 10^{-3} mm^2/s).

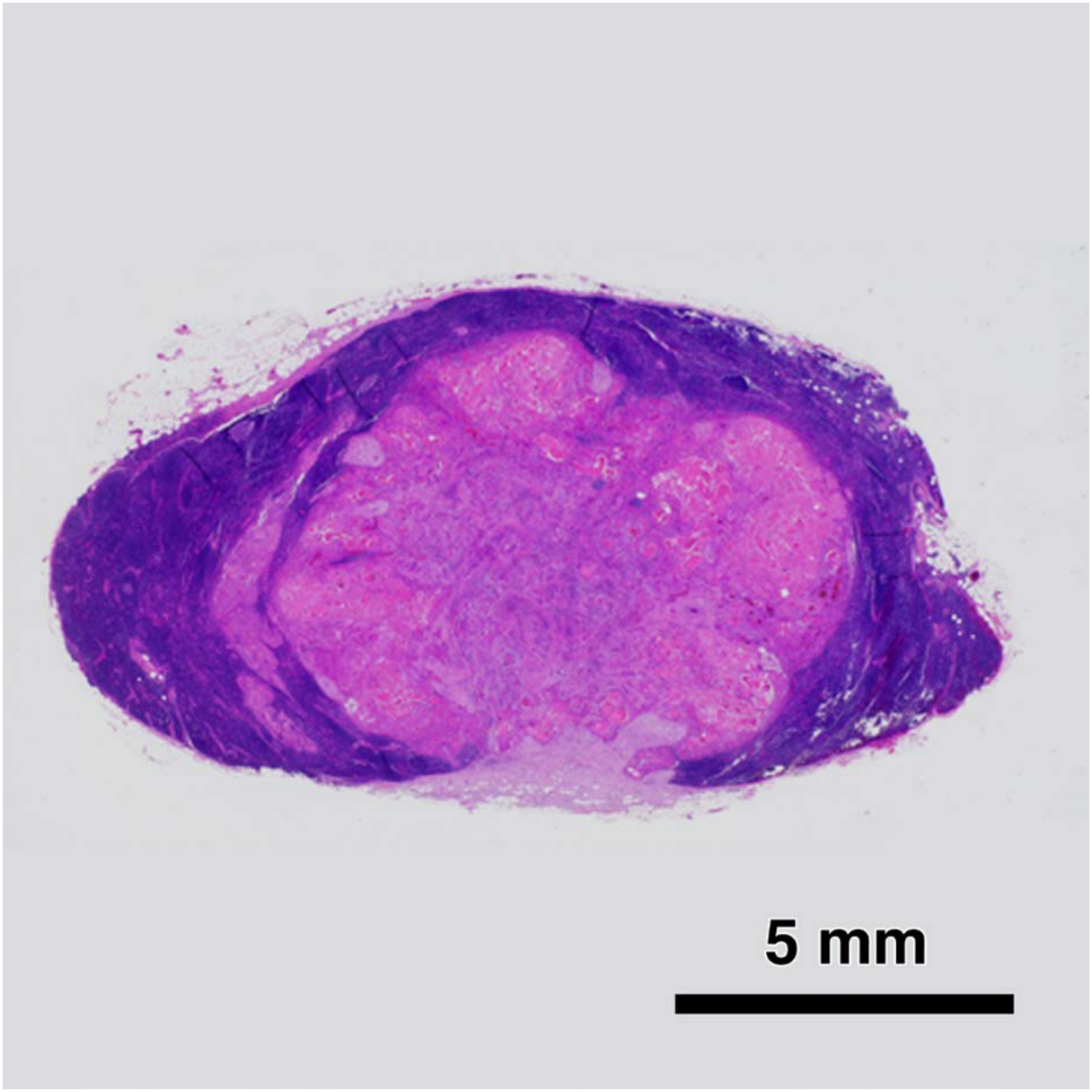

Figure 6. Images of a 66-year-old man with metastatic lymph nodes.
(e) Histopathologic examination shows that the lymph has metastasis of squamous cell carcinoma. (Hematoxylin-eosin stain; original magnification, x10.)

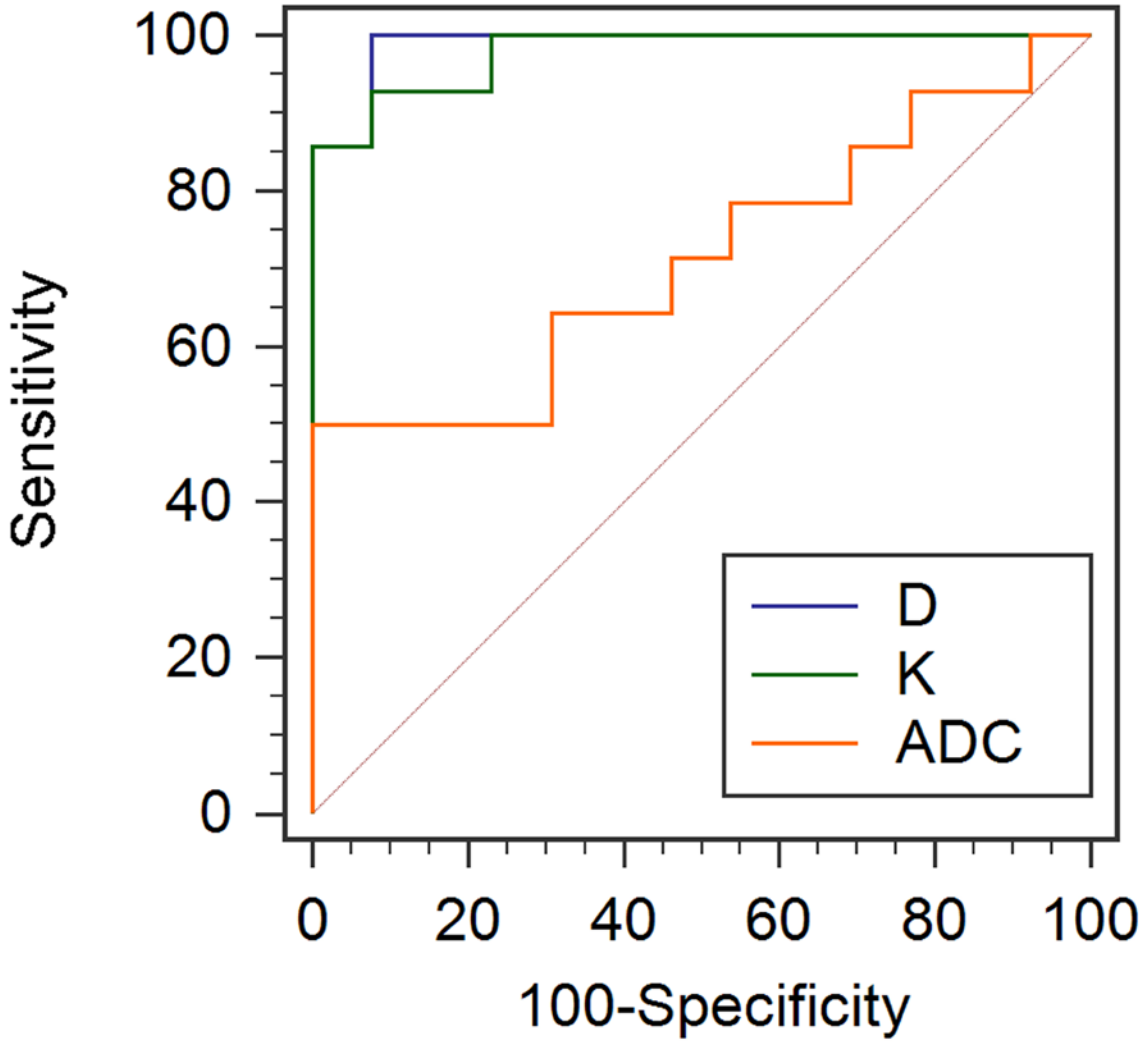

Figure 7. ROC curve analyses of the DKI parameters in patients with oral carcinoma. **(a)** ROC curves for differentiating Grade 2 or Grade 3 from Grade 1 oral carcinomas. The AUCs for D values (0.989; P = 0.0115) and K values (0.978; P = 0.0089) were significantly larger than the AUC for ADC values (0.714). There was no significant difference in the AUCs between the D values and K values (P = 0.6774).

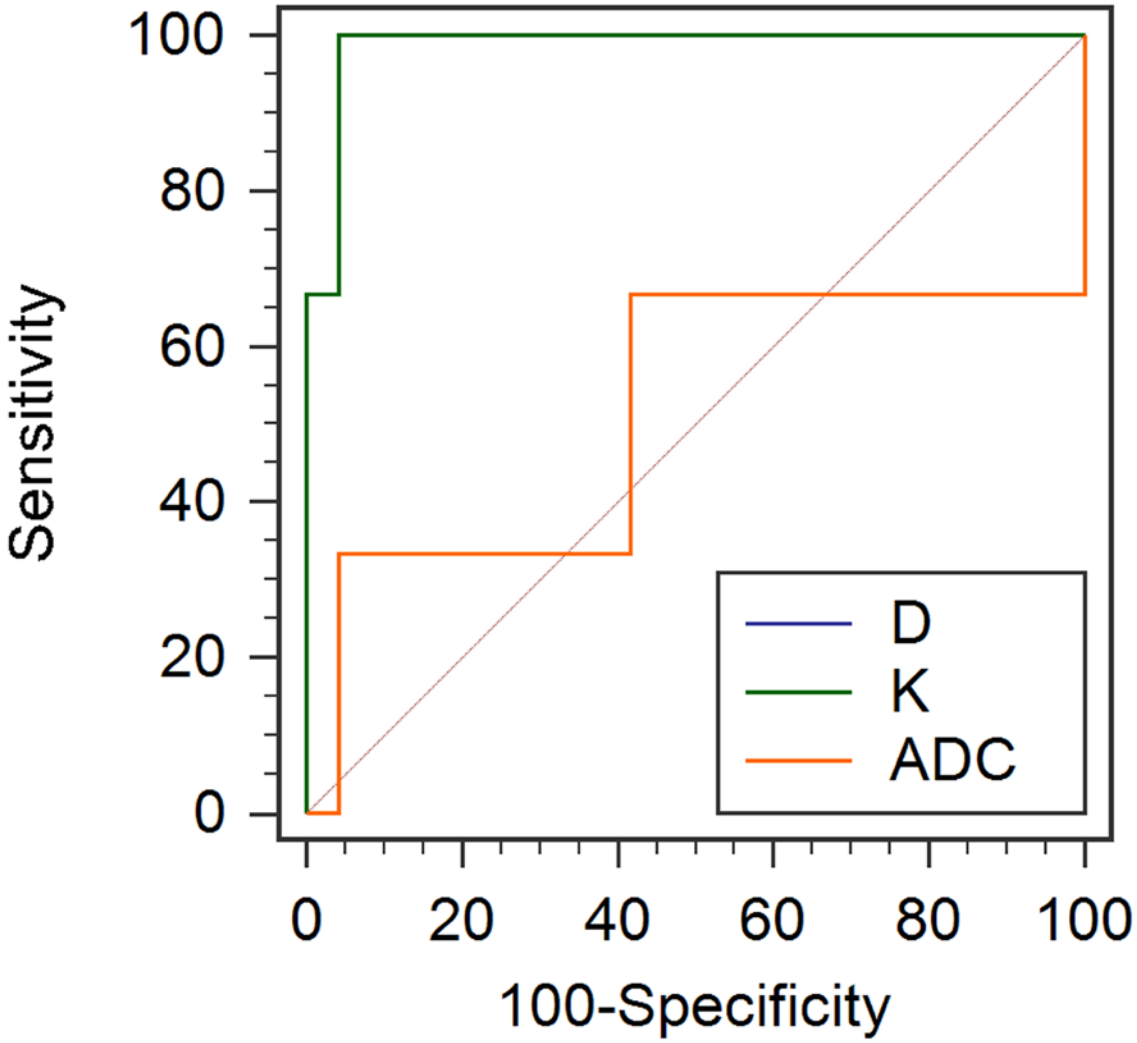

Figure 7. ROC curve analyses of the DKI parameters in patients with oral carcinoma. **(b)** ROC curves for differentiating Grade 3 from Grade 1 or Grade 2 oral carcinomas. The AUCs for D values (0.986; P = 0.0968) and K values (0.986; P = 0.1075) were larger than the AUC for ADC values (0.514), although there was no significant difference).

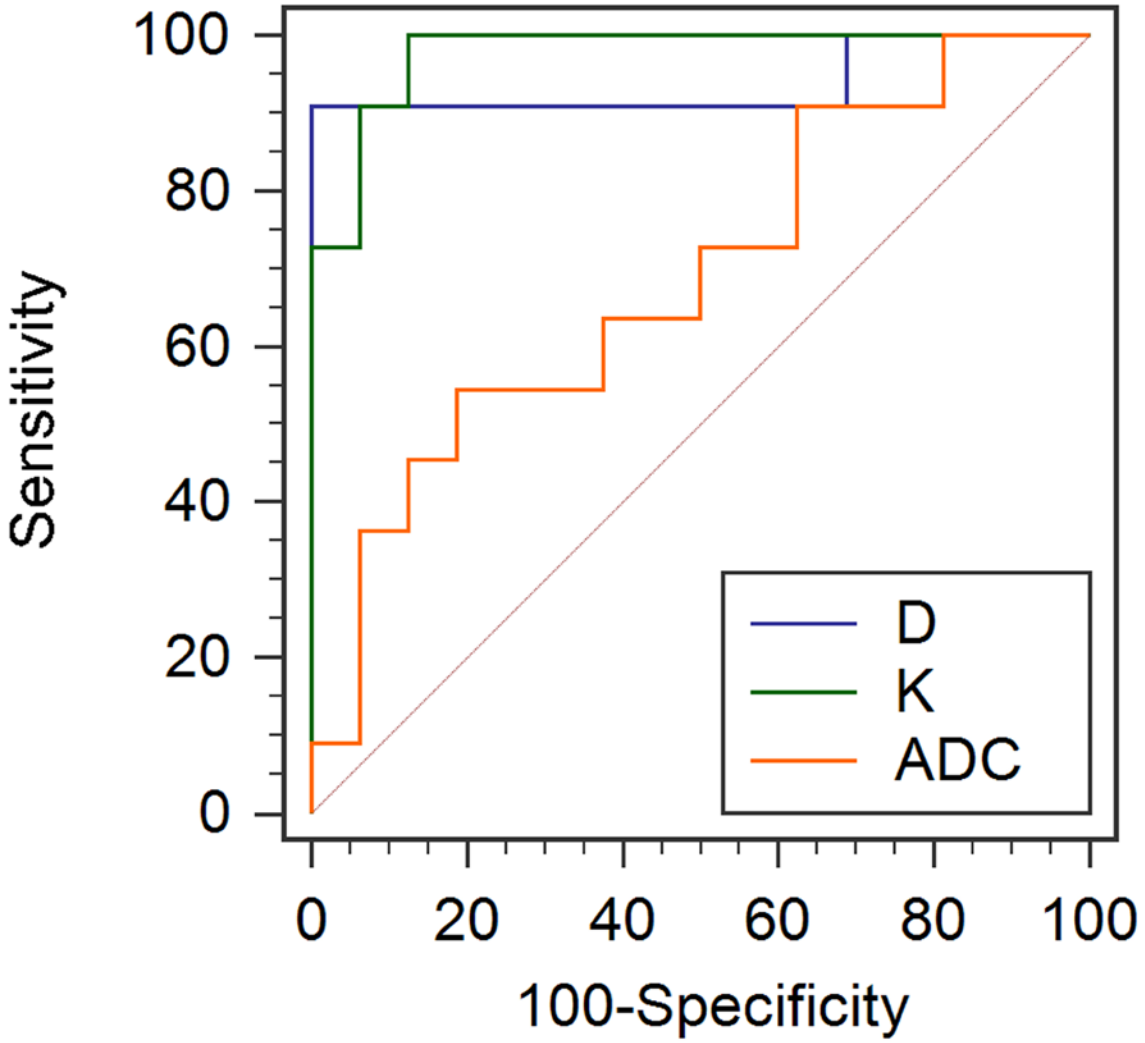

Figure 7. ROC curve analyses of the DKI parameters in patients with oral carcinoma. **(c)** ROC curves for differentiating metastatic from non-metastatic lymph nodes in patients with oral carcinoma. The AUCs for the D values (0.938; P = 0.0132) and the K values (0.977; P = 0.0077) were significantly higher than the AUC for the ADC values (0.688). There was no significant difference in the AUCs between the D values and K values (P = 0.5249).